TI 设计：TIDA-01409
汽车电容式踢脚开启参考设计

TEXAS INSTRUMENTS

说明

该参考设计使用电容式感应技术来检测用户意在打开汽车电动后备箱门、电动行李厢或电动滑动门的踢脚动作。高分辨率和低功率耗散使得该 TI 设计适用于汽车免手动关闭系统，其中姿态检测和低电池电流对该系统来说至关重要。双通道电容数字转换器可接受来自两个传感器的输入，从而支持复杂的动作检测算法和垂直面中的动作识别。

该参考设计采用 LaunchPad™格式，以小型双层板的形式加以实现，具有连接任意 3.3V 微控制器（通过 I²C）和少量通用输入/输出信号的简单接口。该设计由 12V 汽车电池系统直接供电，可以为外部微控制器和所有车载组件创建稳定的 3.3V 电源。

该设计具有适当的保护措施，不受输入电源上电池反向连接等故障的影响，并且能够承受负载突降等情况下发生的高达 40V 的输入电压。车载手动开关可对来自车辆安全系统的"密钥卡已发现"信号的功能进行仿真。

资源

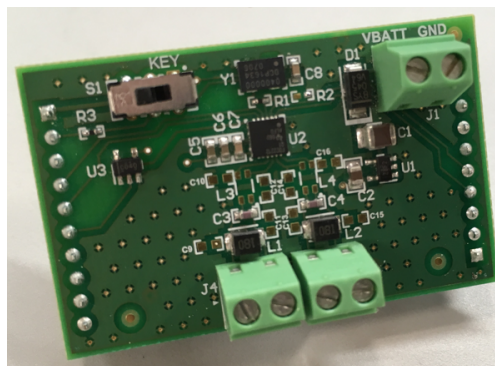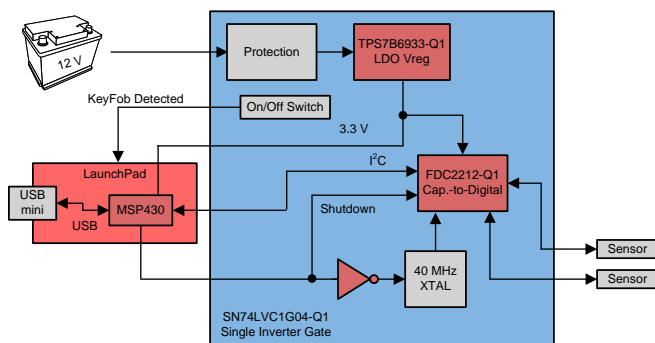|	
TIDA-01409	设计文件夹
FDC2212-Q1	产品文件夹
TPS7B6933-Q1	产品文件夹
SN74LVC1G04-Q1	产品文件夹

TI E2E™ Community　　咨询我们的 E2E 专家

特性

- 两个高分辨率电容式传感器
- 由 12V 汽车电池供电
- 可以在最远 50cm 的距离内检测到踢脚动作
- 低静态电流
- 电池反向保护
- 用于连接微控制器的简单接口
  - I²C 串行通信
  - 可选择的 I²C 地址
  - 中断信号
  - 关断信号
  - 密钥卡信号
- 车载 3.3V 电源

应用

- 汽车后备箱踢脚开启
- 汽车后备箱门踢脚开启
- 汽车滑动门踢脚开启
- 其他免手动汽车 应用

该 TI 参考设计末尾的重要声明表述了授权使用、知识产权问题和其他重要的免责声明和信息。

1 System Description

The Capacitive Kick-to-Open reference design provides a simple implementation of gesture recognition using the dual-channel FDC2212-Q1 capacitive-to-digital converter. When connected to two external capacitive sensors (antennas), this TI Design provides all the analog signal processing to excite the resonant structure of each sensor circuit and to detect changes in the resonant frequency due to changes in the electromagnetic characteristics of the space around the sensors. This sensed data is processed and digitized for each sensor with a 28-bit resolution. The system is flexible to allow for optimization of the gesture detection algorithm based on the digital data from the FDC2212-Q1, which is available as serial data over the I^{2}C communications link.

This TI Design is implemented as a small BoosterPack™ board, with only two layers to keep the design cost-effective. The simple 20-pin interface to an external microcontroller conforms to the LaunchPad 20-pin standard; the testing described in this design guide is performed using an MSP430G2553 LaunchPad with code based on examples already available on TI.com.

The reference design is powered by a standard 12-V automotive battery system and is protected against reverse battery conditions and high voltage up to 40 V as might be experienced during a load dump event. When placed in Shutdown mode, the entire design has an input current less than 100 µA, allowing this design to be connected directly to the battery system without excessive battery current drain.

The components selected for this TI Design are rated for automotive applications.

1.1 *Key System Specifications*

表 **1. Key System Specifications**

PARAMETER	SPECIFICATIONS	DETAILS
Power supply voltage range (operational)	4 to 16 V	节 3.2.1.2
Power supply voltage range (survivable)	–20 to 40 V	节 3.2.1.1
Power supply current (operational)	40 mA	节 3.2.1.4
Power supply current (standby)	100 µA maximum	节 2.4.1.2
Sense range (maximum)	500 mm	节 3.2.4.1
Kick gesture duration	1 to 4 seconds	节 3.2.4
Sense sampling rate	20 to 50 samples per second	节 3.2.4.2
Board layers	2	4.3 节
Form factor	BoosterPack for MSP430™ LaunchPad	节 4.3.1
Microcontroller interface	20-pin LaunchPad format	节 2.4.4

2   System Overview

2.1   *Block Diagram*

图 1 shows the reference design components (in blue), the external capacitive sensors (or "antennas"), the external 12-V automotive battery power supply, and the external MSP430 LaunchPad microcontroller board.
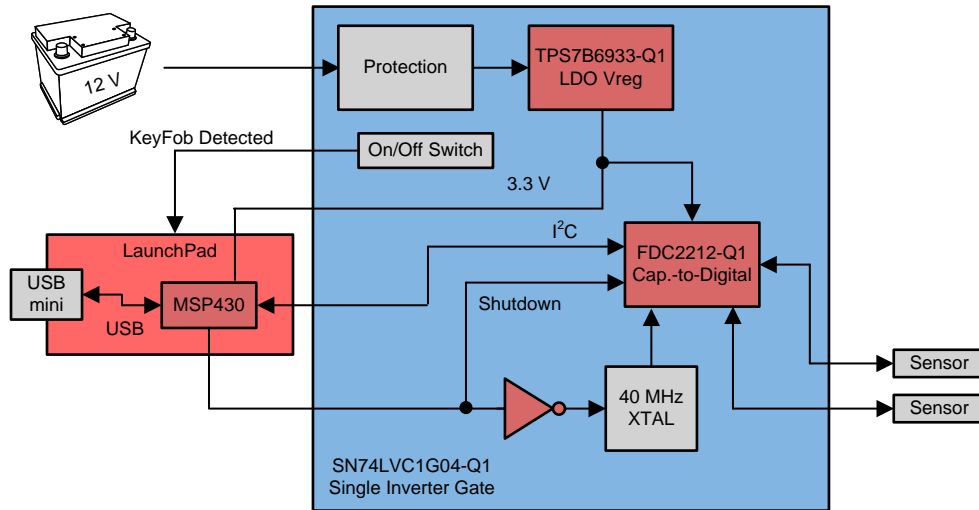
图 **1. TIDA-01409 Block Diagram**

2.2 Highlighted Products

2.2.1 FDC2212-Q1

The FDC2212-Q1 is a two-channel noise- and EMI-resistant, high-resolution, high-speed capacitance-to-digital converter for implementing capacitive sensing solutions. The device employs an innovative narrow-band based architecture to offer high rejection of noise and interferers while providing high resolution at high speed. The device supports a wide excitation frequency range, offering flexibility in system design.

In contrast to traditional switched-capacitance architectures, the FDC2212 employs an LC resonator, also known as LC tank, as a sensor. The narrow-band architecture allows unprecedented EMI immunity and greatly reduced noise floor when compared to other capacitive sensing solutions. Using this approach, a change in capacitance of the LC tank can be observed as a shift in the resonant frequency. Using this principle, the FDC is a capacitance-to-digital converter (FDC) that measures the oscillation frequency of an LC resonator. The device outputs a digital value that is proportional to frequency. This frequency measurement can be converted to an equivalent capacitance.
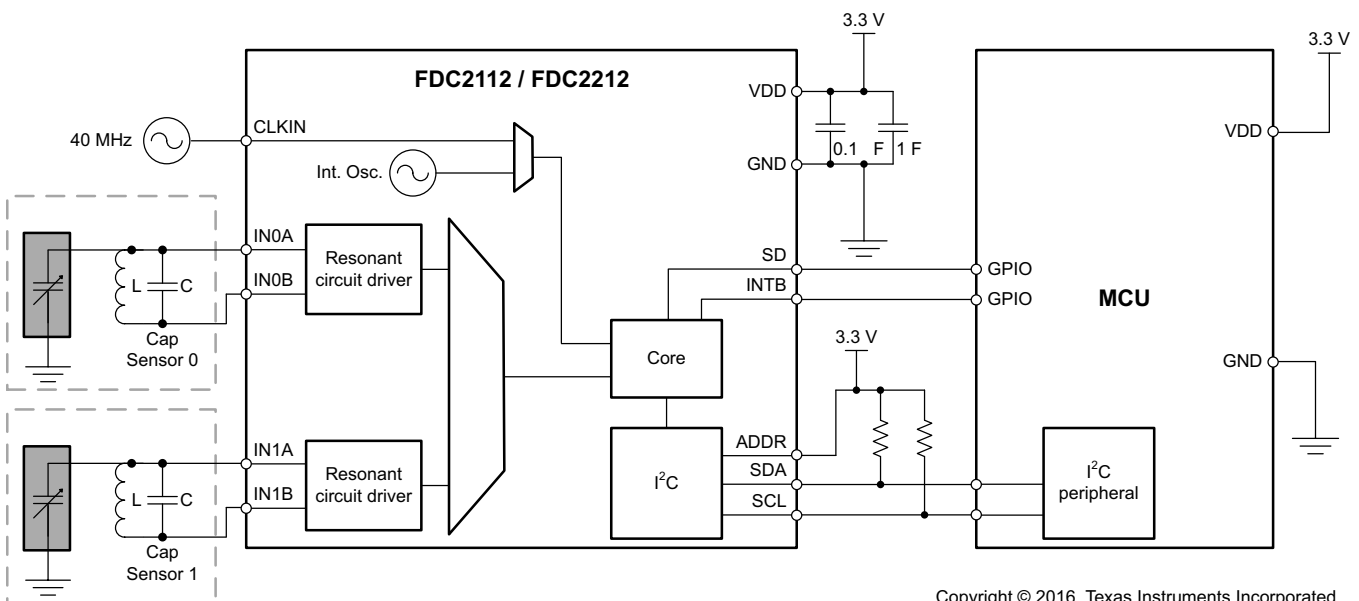
Copyright © 2016, Texas Instruments Incorporated

图 2. Block Diagram of FDC2212

The FDC is composed of front-end resonant circuit drivers, followed by a multiplexer that sequences through the active channels, connecting them to the core that measures and digitizes the sensor frequency (f_{SENSOR}). The core uses a reference frequency (f_{REF}) to measure the sensor frequency. f_{REF} is derived from either an internal reference clock (oscillator), or an externally supplied clock. The digitized output for each channel is proportional to the ratio of f_{SENSOR}/f_{REF}. The I²C interface is used to support device configuration and to transmit the digitized frequency values to a host processor. The FDC can be placed in shutdown mode, saving current, using the SD pin. The INTB pin may be configured to notify the host of changes in system status.

2.2.2   TPS7B6933-Q1

The TPS7B6933-Q1 device is a low-dropout linear regulator designed for up to 40-V input voltage operations. With only a 15-µA (typical) quiescent current at light load, the device is suitable for systems which have a standby-mode, especially in automotive applications. The device featured integrated short-circuit and overcurrent protection. The TPS7B6933-Q1 device operates over a –40°C to 125°C temperature range. Because of these features, the TPS7B6933-Q1 device is well suited in power supplies for various automotive applications.

- Qualified for automotive application
- AEC-Q100 qualified with the following results:
    - Device temperature grade 1: –40°C to 125°C ambient operating temperature range
    - Device HBM ESD Classification Level 2
    - Device CDM ESD Classification Level C4B
- 4- to 40-V wide VI input voltage range with up to 45-V transient
- Maximum output current: 150 mA
- Low quiescent current (I_Q): 15 µA typical at light loads 25 µA maximum under full temperature
- 450-mV typical low dropout voltage at 100-mA load
- Current stable with low ESR ceramic output capacitor (2.2 to 100 µF)
- Fixed 3.3-V output voltage
- Integrated fault protection:
    - Thermal shutdown
    - Short-circuit protection
- 5-pin SOT-23 package

图 3 shows the block diagram of the TPS7B6933-Q1 with the major internal features identified. While only three terminals are shown in the block diagram, the actual component has five pins in this TI Design with two ground pins and one unused pin.

图 3. **Functional Block Diagram of TPS7B6933-Q1**

2.2.3   SN74LVC1G04-Q1

This single inverter gate is designed for 1.65- to 5.5-V VCC operation. The SN74LVC1G04 performs the Boolean function Y = not(A). This device is fully specified for partial-power-down applications using Ioff. The Ioff circuitry disables the outputs, preventing damaging current backflow through the device when it is powered down.

- Qualified for automotive applications
- AEC-Q100 qualified with the following results:
    - Device temperature grade 1: –40°C to 125°C ambient operating temperature range
    - Device HBM ESD Classification Level H2
    - Device CDM ESG Classification Level C4B
- ESD protection exceeds 2000 V per MIL-STD-883, Method 3015; exceeds 200 V using machine model (C = 200 pF, R = 0)
- Supports 5-V VCC operation
- Low-power consumption, 10-µA max ICC
- Inputs accept voltages to 5.5 V
- Max tpd of 3.3 ns at 3.3 V
- ±24-mA output drive at 3.3 V
- Ioff supports partial-power-down mode operation
- Latch-up performance exceeds 100 mA per JESD 78, Class II
- Small package, less than 3 mm × 3 mm

2.2.4   MSP430-Q1

The Texas Instruments MSP430 family of ultra-low-power microcontrollers consists of several devices featuring different sets of peripherals targeted for various applications. The architecture, combined with five low-power modes, is optimized to achieve extended battery life in portable measurement applications. The device features a powerful 16-bit RISC CPU, 16-bit registers, and constant generators that contribute to maximum code efficiency. The digitally controlled oscillator (DCO) allows the device to wake up from low-power modes to active mode in less than 1 µs. The MSP430G2x53 series are ultra-low-power mixed signal microcontrollers with built-in 16-bit timers, up to 24 I/O capacitive-touch enabled pins, a versatile analog comparator, a 10-bit analog-to-digital (A/D) converter, and built-in communication capability using the universal serial communication interface. Typical applications include low-cost sensor systems that capture analog signals, convert them to digital values, and then process the data for display or for transmission to a host system.

- Qualified for automotive applications

- Low supply-voltage range: 1.8 to 3.6 V

- Ultra-low-power consumption

    – Active mode: 230 µA at 1 MHz, 2.2 V

    – Standby mode: 0.5 µA

    – Off mode (RAM retention): 0.1 µA

- Five power-saving modes

- Ultra-fast wakeup from standby mode in less than 1 µs

- 16-bit RISC architecture, 62.5-ns instruction cycle time

- Universal serial communication interface (USCI)

    – Enhanced UART supports automatic baud-rate detection (LIN)

    – IrDA encoder and decoder

    – Synchronous SPI

    – I^{2}C

- On-chip comparator for analog signal compare function or slope analog-to-digital (A/D) conversion

- 10-bit, 200-ksps, analog-to-digital converter (ADC) with internal reference, sample-and-hold, and autoscan
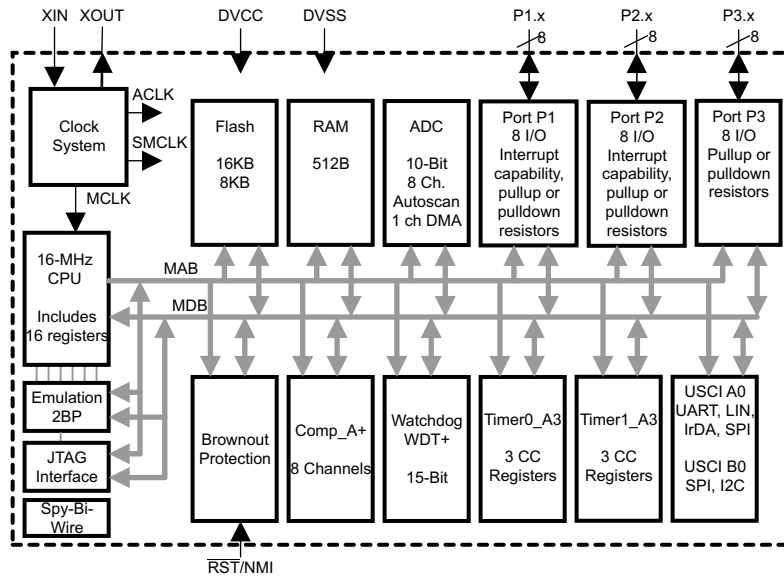
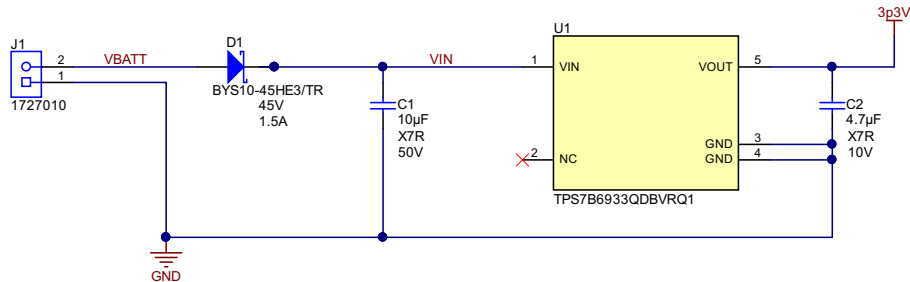图 **4. Functional Block Diagram of MSP430G2-Q1**

2.3   Design Considerations

To simplify this reference design, and make it more adaptable to a variety of microcontrollers, the board was implemented in the BoosterPack format. This board format has a simple connector interface to the external LaunchPad microcontroller board, allowing evaluation of the Capacitive Kick-to-Open reference design with a wide selection of microcontrollers. The LaunchPad plus BoosterPack implementation also has the advantage that code development and design testing are facilitated by existing tools such as Code Composer Studio™, thus speeding up optimization of the design for any specific operating conditions.

While the BoosterPack format does allow flexibility in using different microcontroller boards, it also creates constraints on the size and layout of the TIDA-01409 board. In a production version of this design, the microcontroller would likely be installed on the same board with the FDC2212-Q1 and other components, with a possible reduction in board size.

2.4   System Design Theory

2.4.1   Power Supply

The power supply converts the 12-V automotive battery voltage to the 3.3-V supply needed by the microcontroller, FDC2212-Q1 Capacitive-to-Digital Converter, the SN74LVC1G04-Q1 logic inverter and the other components. The requirements for the power supply circuit are to produce a stable 3.3-V supply capable of at least 35 mA, while surviving electrical conditions such as reverse-battery and load-dump. 图 5 shows the electrical schematic of the power supply circuit.
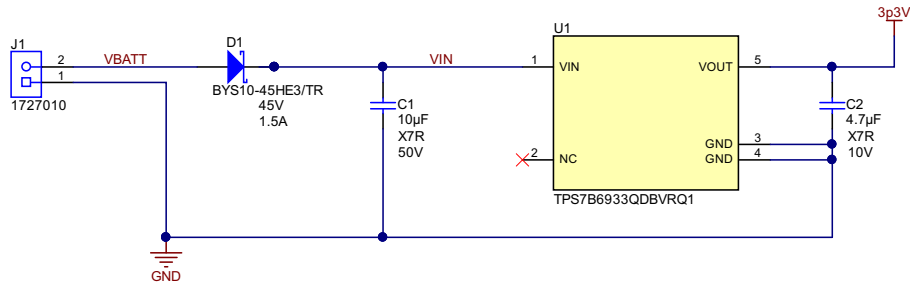
Copyright © 2017, Texas Instruments Incorporated

图 5. Power Supply Electrical Schematic

Diode D1 provides protection against reverse-battery conditions. The BYS10-45 Schottky Barrier Rectifier was selected because it has a low forward voltage of less than 400 mV (at 25°C) and a reverse breakdown voltage of 45 V. It is also AEC-Q101 qualified for automotive applications.

The TPS7B6933-Q1 provides regulation of a fixed 3.3-V supply and has a wide survivable input voltage range up to 45 V. It is stable with ceramic output capacitors, which is preferred for automotive applications.

2.4.1.1   Operation With Low Input Voltage

The TPS7B6933-Q1 has a maximum dropout voltage of 800 mV. Combined with the forward voltage of the BYS10-45, this means the Capacitive Kick-to-Open reference design operates down to input voltages of: Minimum operating voltage = 3.3 V + 400 mV + 800 mV = 4.5 V.

While it is not expected that the Kick-to-Open feature would be used during "start/stop" conditions, this relatively low minimum operating voltage does give comfortable margin for the expected conditions for its typical applications.

2.4.1.2   Low Supply Current in Standby Mode

One requirement for this Capacitive Kick-to-Open reference design is to have low quiescent current when the kick-to-open feature is not in active use. This is critical to prevent excessive current draw from the automotive battery during long periods when the vehicle is idle.

表 2. Current Consumption in Standby

DEVICE	TYPICAL QUIESCENT CURRENT (µA)	MAXIMUM QUIESCENT CURRENT (µA)	COMMENT
TPS7B6933-Q1	15.0	25.0	—
FDC2212-Q1	36.0	60.0	—
SN74LVC1G04-Q1	< 10.0	10.0	—
MSP430G2553-Q1	56.0	—	Low-power mode 0
	22.0	—	Low-power mode 2
	0.7	1.5	Low-power mode 3
DSC1001BI1-040	15.0	—	Standby mode

2.4.2   Capacitive-to-Digital Converter

图 6 shows the electrical schematic for the capacitive-to-digital converter circuit. This reference design includes two channels of resonant LC circuits, which can be used to sense two independent capacitive sensors. For one channel, L1 and C3 form the primary LC tank circuit, which has a resonant frequency, determined not only by the values of L1 and C3, but also by the effective capacitance of the sense element (antenna) connected to connector J4. The FDC2212-Q1 then uses a high-frequency clock to determine the resonant value of L1 in parallel with the total capacitance. The resonant frequency is:

$$f_{resonant} = \frac{1}{\left(2 \times \pi \times \sqrt{L1 \times \left(C3 + C_{antenna}\right)}\right)}$$

(1)

which for the values shown give a resonant frequency of 6.5 MHz. As additional capacitance is sensed on the external antenna, the total capacitance increases, and the resonant frequency decreases.
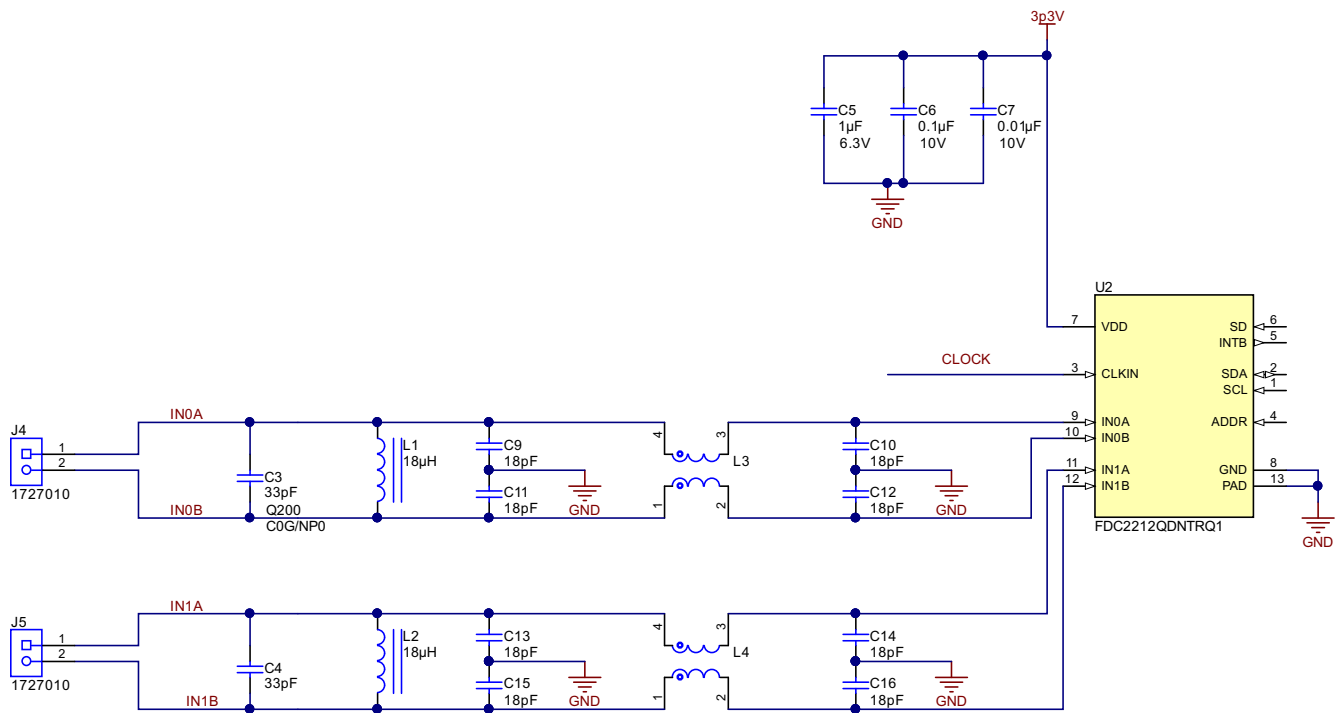
图 **6. Capacitive-to-Digital Converter Electrical Schematic**

As discussed in the *FDC2114 and FDC2214 EVM User's Guide*[2], C9, C11, C13, and C15 are intended to be installed to reduce EMI emissions issues, especially in the case where long sensor wires (antennas) are used. Similarly, C10, C12, C14, and C16 are intended to be installed to reduce EMI susceptibility issues, especially where long sensor wires are used. Likewise, the common-mode chokes L3 and L4 are optional to reduce EMI issues due to high-frequency transitions.

Capacitors C5, C6, and C7 are provided to decouple the FDC2212-Q1 from the 3.3-V power supply. These capacitors serve to provide short-term smoothing of the supply to the FDC2212-Q1 in the case of brief voltage transients on the 3.3-V supply and during short surges in the current draw of the FDC2212-Q1 device.

2.4.3 Oscillator

The FDC2212-Q1 uses a high-frequency oscillator as a clock reference to determine the timing of the resonant LC circuit, which forms the capacitive sensor. The FDC2212-Q1 has an internal oscillator that can be used for this purpose, but the accuracy of measurements is improved with an external precision oscillator. The DSC1001BI1-040 oscillator is a silicon MEMS-based CMOS oscillator offering excellent jitter and stability performance over a wide range of supply voltages and temperatures. The device operates at 40 MHz from a 3.3-V supply and a temperature range of –40ºC to 85ºC.

The resistors R1 and R2 allow configuration of this reference design with either the internal oscillator of the FDC2212-Q1 (with R2 installed and R1 not installed) or with the precision oscillator Y1 (with R1 installed and R2 not installed). A logic inverter U3 is required because the Shutdown signal must have a positive logic (HIGH = Shutdown) for the FDC2212-Q1, but a negative logic (LOW = Shutdown) is required by the DSC1001 oscillator device. 图 7 shows the electrical schematic of the oscillator portion of the reference design.

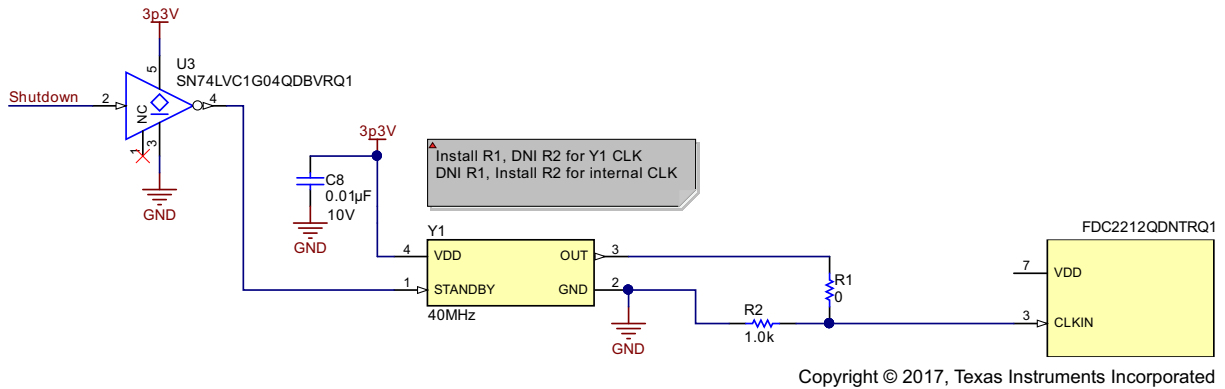Copyright © 2017, Texas Instruments Incorporated

图 7. Oscillator Electrical Schematic

The advantage of using the external oscillator is the higher precision of capacitive measurements, due to the more stable oscillator frequency. The comparison between these two oscillator options is shown in 表 3. Due to the nature of the Capacitive Kick-to-Open application, the absolute precision of the measurement is not critical; the kick-to-open detection algorithm is more dependent on relative measures of changing capacitance over a short interval (a few seconds) than any long-term measurement or comparison to an absolute capacitance standard. Therefore, designers may consider whether using the internal oscillator is a viable option, trading reduced precision for a reduction in module bill of materials and cost.

表 3. Comparison of Oscillator Precision

PARAMETER	FDC2212-Q1 INTERNAL OSCILLATOR	DSC1001BI1-040 PRECISION OSCILLATOR
Nominal frequency (MHz)	43.4	40
Frequency tolerance (ppm)	±250000	±50
Temperature coefficient	−13 ppm/°C	Included in ±50 ppm
Aging tolerance (ppm)	—	±5

2.4.4 Microcontroller Interface

图 8 shows the electrical schematic of the interface between the TIDA-01409 Capacitive Kick-to-Open board and the LaunchPad microcontroller board. This interface complies with the LaunchPad and BoosterPack format, and allows evaluation of the TIDA-01409 Capacitive Kick-to-Open board with a variety of microcontrollers. Due to the simplicity of the I²C interface between the microcontroller and the FDC2212-Q1, there are very few pins used to make the connections to the TIDA-01409 circuits.
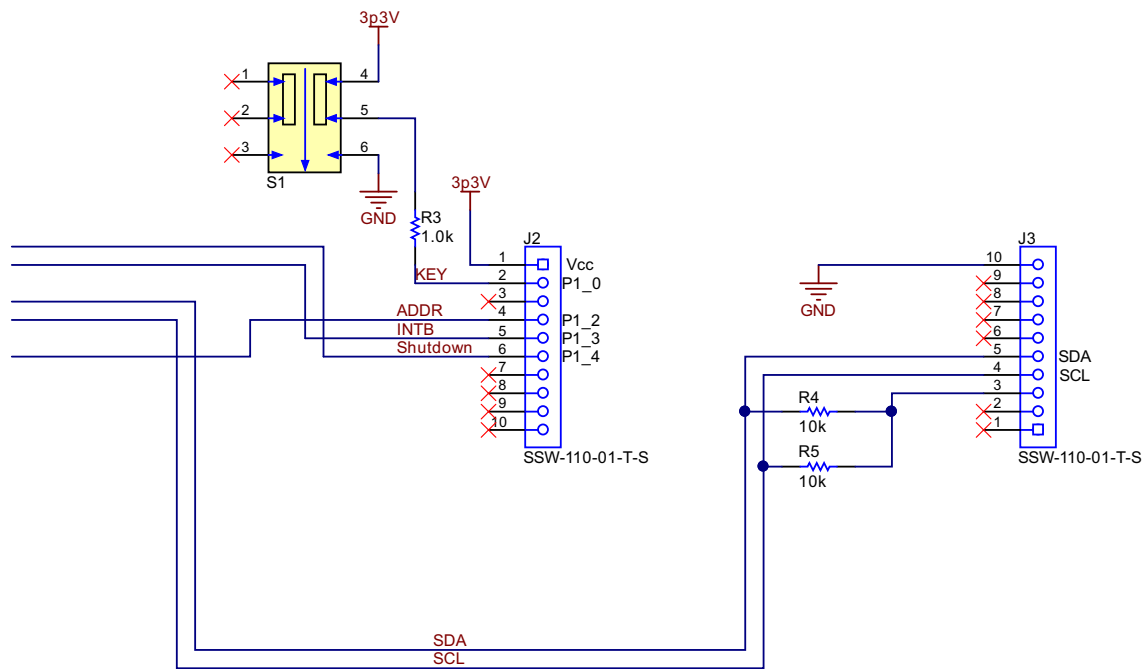
Copyright © 2017, Texas Instruments Incorporated

图 **8. Microcontroller Interface Electrical Schematic**

The LaunchPad microcontroller board is powered by the 3.3-V supply (J2-1) generated on the TIDA-01409 board, with respect to the common ground for both boards (J3-10). Because the voltage regulator on the TIDA-01409 board can supply up to 150 mA at 3.3 V, this allows a wide variety of microcontrollers such as the MSP430 or C2000™ families to be evaluated with the Capacitive Kick-to-Open reference design.

The I²C interface is connected on pins J3-4 (Serial Clock SCL) and J3-5 (Serial Data SDA). R4 and R5 are pullup resistors and are enabled by setting P3-3 to a logic high state when communication between the microcontroller and the FDC2212-Q1 is desired.

Switch S1 is used to emulate the function of a "key fob detected" signal from the vehicle security system. This switch allows designers to test that the kick-to-open operation is only enabled when the key fob is within range and correctly identified. The microcontroller software must be written such that no kick-to-open operation occurs when the KEY signal on GPIO Port 1.0 indicates no valid key fob is detected.

The ADDR signal on J2-4 (GPIO P1.2) allows designers to change the address of the FDC2212-Q1 between 0x2A when ADDR is logic LOW and 0x2B when ADDR is logic HIGH. This feature allows for having two independent FDC2212-Q1 devices with communication to a common microcontroller using the same I²C interface, by addressing the separate FDC2212-Q1 devices differently.

The INTB signal on J2-5 (GPIO P1.3) is a configurable interrupt signal from the FDC2212-Q1 to the microcontroller. It can be used to signal the microcontroller that an updated measurement is available in the FDC2212-Q1 registers.

The Shutdown signal on J2-6 (GPIO P1.4) allows the microcontroller to put the FDC2212-Q1 and the oscillator into a low-power standby mode. This is useful during long periods of inactivity to reduce current consumption from the vehicle battery. In operation, the microcontroller could be in a low-power mode with periodic brief intervals of monitoring the KEY signal, with no need to activate the rest of the Capacitive Kick-to-Open circuits until a valid key fob is detected.

3 Hardware, Software, Testing Requirements, and Test Results

3.1 Required Hardware and Software

3.1.1 Hardware

The TIDA-01409 Capacitive Kick-to-Open board is installed as a BoosterPack on a LaunchPad microcontroller board to form a complete kick-to-open sensor module. The TIDA-01409 connectors J2 and J3 are 10-pin female connectors installed on the bottom side of the board. These connectors mate to the standard LaunchPad connectors, aligning with the two 10-pin male connector pins on boards such as the MSP430G2553 LaunchPad or with the two outside rows of the two 20-pin male connectors on the LaunchPad XL interface on boards such as the MSP430F5529 LaunchPad. 图 9 shows the TIDA-01409 board correctly mounted on an MSP430G2553 LaunchPad board.
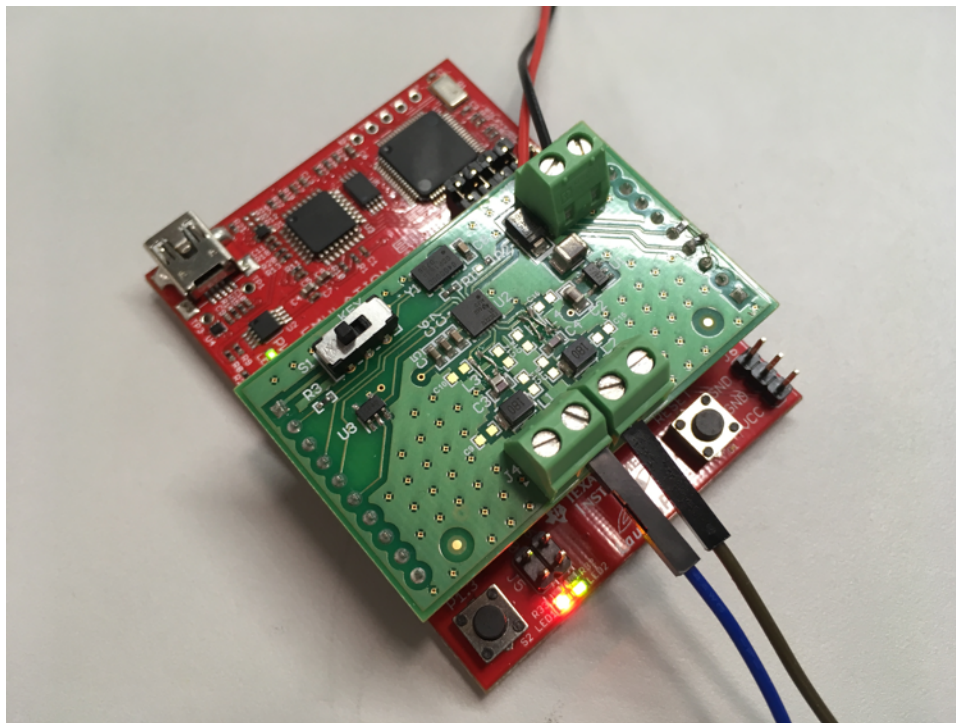
图 9. TIDA-01409 and MSP430G2553 LaunchPad Board

When installing the TIDA-01330 board on the LaunchPad board, make sure to alight all ten sockets of each of the two 10-contact headers with the corresponding pins on the LaunchPad board. The orientation is such that the USB connector on the LaunchPad board will be on the same side as switch S1 on the TIDA-01409 board.

3.1.2 Software

Software must be loaded to the LaunchPad microcontroller board to control the function of the TIDA-01409 Capacitive Kick-to-Open board. 图 10 shows a simplified flow chart for the reference design. Designers tailor these functional blocks to best fit the requirements of the specific applications they are addressing.
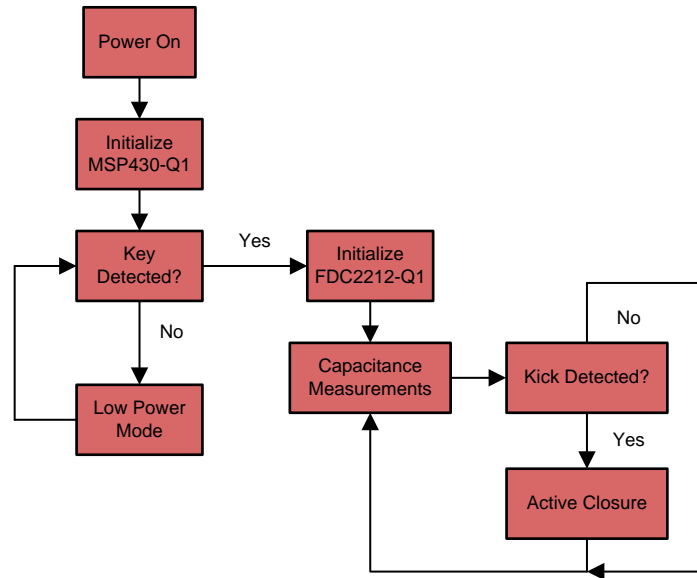
图 **10. Simplified Flow for Capacitive Kick-to-Open**

3.1.2.1 Power On

When 12-V power is applied to VBATT (J1-2) with respect to GND (J1-1), the TPS7B6933-Q1 regulates the input voltage to produce a 3.3-V output voltage; no enable or signal is required. The 3.3-V supply (3p3V) is then applied to the FDC2212-Q1 and other components on the TIDA-01409 board as well as to the MSP430 LaunchPad board through connectors J2 and J3.

When the FDC2212-Q1 powers up, it enters into sleep mode and waits for configuration. Once the device is configured, it exits sleep mode when the I²C communication from the LaunchPad causes CONFIG.SLEEP_MODE_EN to be set to binary 0. TI recommends configuring the FDC while in sleep mode. If a setting on the FDC needs to be changed, return the device to sleep mode, change the appropriate register, and then exit sleep mode.

3.1.2.2 Initialize Microcontroller

After 3.3-V power is applied to the LaunchPad, the microcontroller must be configured. This configuration involves setting up the GPIO ports to the appropriate input and output conditions and enabling I²C communication with the FDC2212-Q1.

The GPIO pins corresponding to the MSP430G2553 LaunchPad are noted on the TIDA-01409 electrical schematic. These are also listed in 表 4. If a different microcontroller board is used, similar signal connections are required, but the specific port and GPIO assignments may be different.

As part of the microcontroller initialization step, these GPIO and I²C pins must be configured for the proper function and direction. See the User's Guide for the specific LaunchPad board being used.

表 4. MCU Connections for MSP430G2553 LaunchPad

SIGNAL	TIDA-01409 PIN	MSP430G2553 LAUNCHPAD	SIGNAL DIRECTION
KEY	J2-2	P1.0	From TIDA-01409 to LaunchPad
ADDR	J2-4	P1.2	From LaunchPad to TIDA-01409
INTB	J2-5	P1.3	From TIDA-01409 to LaunchPad
Shutdown	J2-6	P1.4	From LaunchPad to TIDA-01409
Pullup	J3-3	P2.5	From LaunchPad to TIDA-01409
SCL	J3-4	P1.6	From LaunchPad to TIDA-01409
SDA	J3-5	P1.7	Bidirectional between LaunchPad and TIDA-01409

3.1.2.3   Low Power Mode

Until a key fob is detected, as indicated by the KEY signal, the microcontroller keeps the FDC2212-Q1 and 40-MHz oscillator turned off by asserting the Shutdown signal. The microcontroller can remain in one of its low-power modes for a majority of the time, checking periodically for an assertion of the KEY signal.

3.1.2.4   Initialize FDC2212-Q1

When a key fob is detected, as indicated by a logic HIGH on the KEY signal, the microcontroller de-asserts the Shutdown signal, and the FDC2212-Q1 transitions from Shutdown Mode to Sleep Mode. This transition in the Shutdown signal also enables the 40-MHz oscillator (if installed) to provide a precision clock to the FDC2212-Q1. The microcontroller then configures the FDC2212-Q1 registers by communication through the I^{2}C serial port (see Section 17 of the *MSP430x2xx Family User's Guide*[7]). The specifics of the register settings are given in the FDC2212-Q1 datasheet[1]; 表 5 lists the registers that must be configured before the FDC2212-Q1 is made to exit Sleep Mode.

After the FDC2212-Q1 registers are configured, the device is made to switch from Sleep Mode to Normal Mode by changing the SLEEP_MODE_EN bit of the CONFIG register to binary 0.

表 5. FDC2212-Q1 Registers to Set During Initialization

ADDRESS	NAME	DESCRIPTION
0x08	RCOUNT_CH0	Reference count setting for channel 0
0x09	RCOUNT_CH1	Reference count setting for channel 1
0x10	SETTLECOUNT_CH0	Settling count for channel 0
0x11	SETTLECOUNT_CH1	Settling count for channel 1
0x14	CLOCK_DIVIDERS_CH0	Reference divider settings for Channel 0
0x15	CLOCK_DIVIDERS_CH1	Reference divider settings for Channel 1
0x19	STATUS_CONFIG	Device status reporting configuration
0x1A	CONFIG	Conversion configuration
0x1B	MUX_CONFIG	Channel multiplexing configuration
0x1E	DRIVE_CURRENT_CH0	Channel 0 sensor current drive configuration
0x1F	DRIVE_CURRENT_CH1	Channel 1 sensor current drive configuration

3.1.2.5 *Capacitance Measurements*

When operating in the normal (conversion) mode, the FDC2212-Q1 is periodically sampling the frequency of the sensors and generating sample outputs for the active channels. The measurements are stored in registers DATA_CH0 and DATA_LSB_CH0 for channel 0, and DATA_CH1 and DATA_LSB_CH1 for channel 1. Because the I²C communications transfer data from only one register at a time, reading the data from each channel requires two I²C read commands.

3.1.2.6 *Kick Detected*

After a sequence of measurements has been read from the FDC2212-Q1, the microcontroller determines if a kick gesture has been detected or not. The criteria for whether to declare a valid kick depends on the specifics of the actual vehicle and sensor configuration. In general, consider several factors when making the determination of a valid kick:

- Background measurement before kick
- Variation in repeated measurements before kick
- Direction (increase or decrease) in measurements during kick
- Amplitude of difference between no-kick and kick measurements
- Duration of kicking gesture
- Difference between multiple sensors located at different points on the vehicle

3.1.2.7 *Activate Closure*

If it is determined that a valid kick gesture has been detected, the Capacitive Kick-to-Open board sends a signal to the associated closure system (lift-gate, trunk, sliding door) to activate the desired motor, and thus open or close the mechanism. After the mechanism has moved, the Capacitive Kick-to-Open continues to make capacitive measurements until another kick is detected, the key fob is no longer present, or power to this subsystem is turned off.

3.2 Testing and Results

Unless otherwise noted, the following tests were performed at room temperature, with a 12-V nominal supply. The capacitive sensor data (when applicable) was read from the FDC2212-Q1 registers through the serial port. In some cases, comparison data for different environmental conditions was collected using the graphical user interface (GUI) with the FDC2x14EVM.

3.2.1 Power Supply Testing

The Capacitive Kick-to-Open reference design board is designed to operate from a typical automotive 12-V battery electrical system. As such, it survives events such as high voltage due to load dump and faults such as reverse battery voltage. The board operates over a wide range of input voltages.

3.2.1.1 Survivable Input Voltage Range

图 11 shows the input current from the automotive battery system (VBATT) for a wide range of voltages applied at J1-2 (VBATT) with respect to J1-1 (GND). For these measurements, the Shutdown pin (J2-6) was connected to GND, disabling the Shutdown (low current) feature. These measurements are for the TIDA-01409 board without connection to any LaunchPad microcontroller board.

For reverse-battery conditions (VBATT < 0), there is no significant current for negative voltages up to –20 V. This indicates the reverse-battery blocking diode (D1) is correctly blocking any negative voltages.

For positive VBATT conditions up to 35 V, the input current does not exceed 7 mA, showing the board operating current as expected. At an input voltage of 40 V, the input current increases very slightly, indicating a small increase in leakage current through the devices, but this is not a significant increase, and no damage or faults occurred.
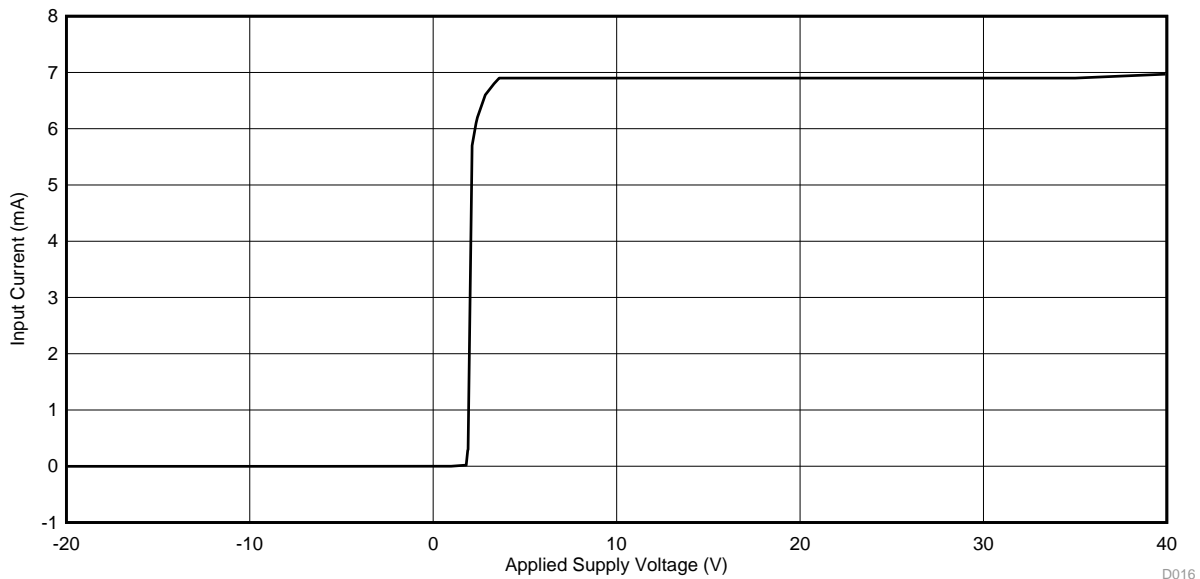
图 **11. Input Current at J1-2 versus Applied Voltage on VBATT**

3.2.1.2   *Operational Input Voltage Range*

Operating the Capacitive Kick-to-Open design is demonstrated for VBATT voltages from 4 to 20 V. 图 12 and 图 13 show the communication between the microcontroller on the LaunchPad board and the FDC2212-Q1 Capacitive-to-Digital Converter on the TIDA-01409 board with the input supply VBATT set to 4 and 20 V, respectively. These figures illustrate that the function of the board is operating over this wide range of supply voltage; a more detailed look at the I²C communication is given in 节 3.2.2.

Unless otherwise specified in the following tests, the VBATT supply was set to 12 V for the measurements of design performance.
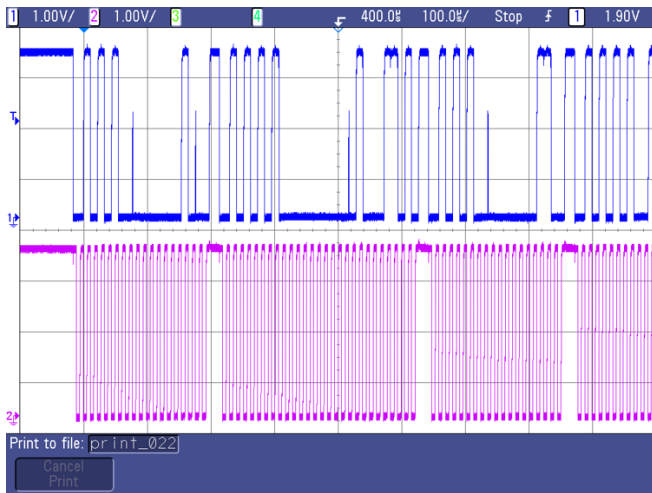
图 12. I²C Communication Between FDC2212-Q1 and Microcontroller With VBATT = 4 V
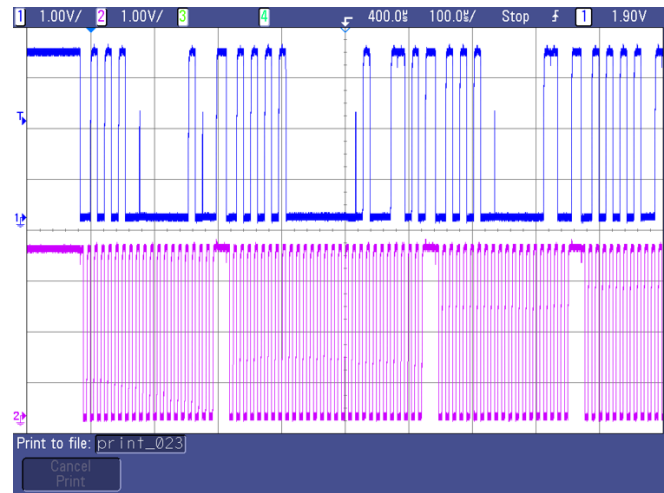
图 13. I²C Communication Between FDC2212-Q1 and Microcontroller With VBATT = 20 V

3.2.1.3   *3.3-V Supply Regulation*

图 14 shows the output of the 3.3-V linear regulator for a wide range of input voltages applied at VBATT. The 3.3-V supply maintains regulation for input across the voltage range from 4 to 40 V.
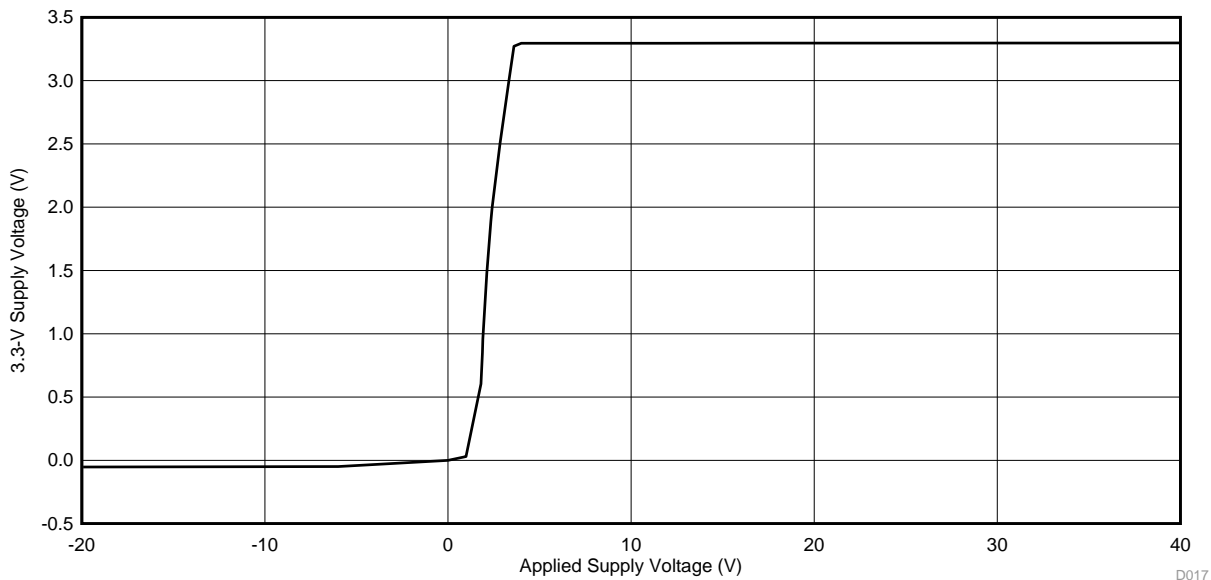
图 14. 3.3-V Supply Voltage versus VBATT Applied Power

3.2.1.4 *Power Consumption*

With 12 V applied to the VBATT connector, and with no LaunchPad connected, the current consumption is 6.8 mA with the Shutdown pin (J2-6) connected to GND (J3-10). The current consumption is reduced to less than 100 µA when the Shutdown pin is connected to 3p3V (J2-1).

During operational testing with the TIDA-01409 connected to an MSP430G2553 LaunchPad board, the input current from VBATT ranged from 26 to 33 mA, including the current supplied by the 3.3-V linear regulator to the LaunchPad microcontroller board. This current varies from 26 to 33 mA primarily due to the illumination (or not) of the LED indicators on the microcontroller board.

3.2.2 I²C Communications

图 15 shows an oscilloscope capture of I²C serial communication between the microcontroller and the FDC2212-Q1. The pink trace (channel 1) is the SCL serial clock signal. Visible in 图 15 is the end of one message, followed by a complete message, with the separation between the two messages indicated by the brief period of logic HIGH on the SCL signal. The FDC2212-Q1 accepts I²C communication rates of 10 to 400 kHz. The clock rate in this example is 6 clocks per 100-µs divisions, or about 60 kHz.

The blue trace (channel 2) is the SDA serial data signal. SDA is pulled up by resistor R4, and actively pulled down by either the I²C master (the microcontroller) or the I²C slave (the FDC2212-Q1). The SDA signal is sampled on the rising edge of the SCL signal. After each 9 bits of address or data are transmitted, the sending node releases the SDA signal and the receiving node pulls SDA low as an acknowledge (ACK) bit. This can be observed in the blue trace in 图 15 where there is a half-size pulse three times in the message, indicating 3 bytes of information are being communicated.
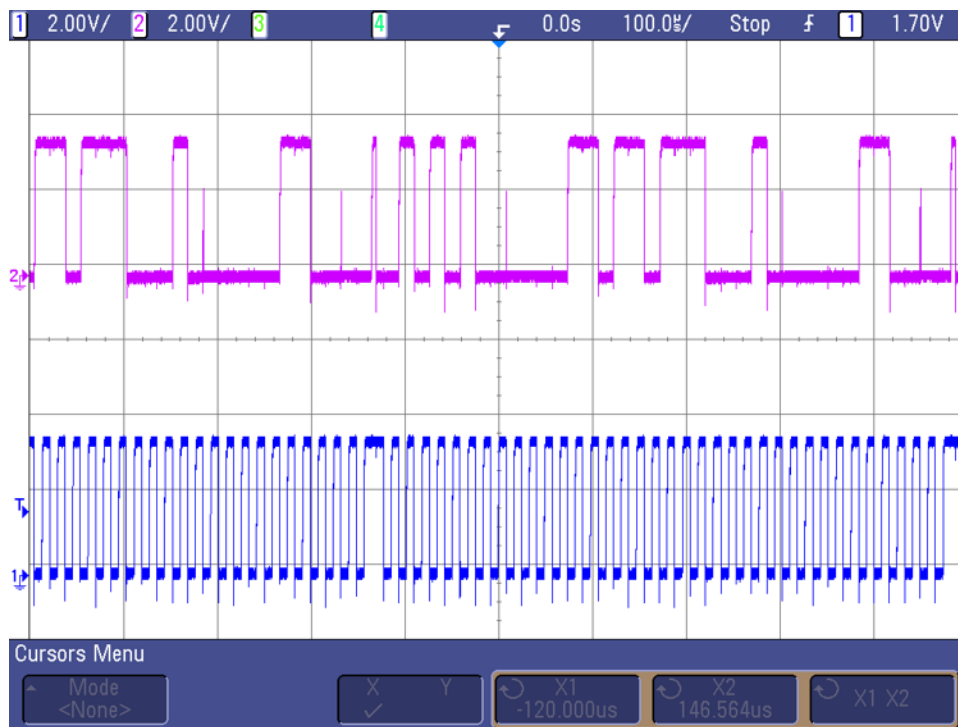

图 **15. I²C Communication Showing SDA Signal (Pink) and SCL Signal (Blue)**

3.2.3 Parametric Adjustment

The FDC2212-Q1 output signals INxA and INxB (where x represents the channel number 0 or 1) excite the LC (inductor - capacitor) "tank" circuit at the resonant frequency. 图 16 shows these signals when the LC resonant circuit has a frequency of 5.1 MHz. The shape and amplitude of the resonant oscillation for each sensor channel is determined by the inductance and capacitance of the hardware, and also by the excitation parameter settings determined by the values stored in the FDC2212-Q1 registers. The registers are listed in 表 5, when properly set, the output waveforms will be similar to 图 16, with the two phases INxA and INxB giving two half-wave sinusoids, a phase difference of 180°, and an amplitude between 1.2 and 1.8 V (the amplitude in 图 16 is actually larger than desired).
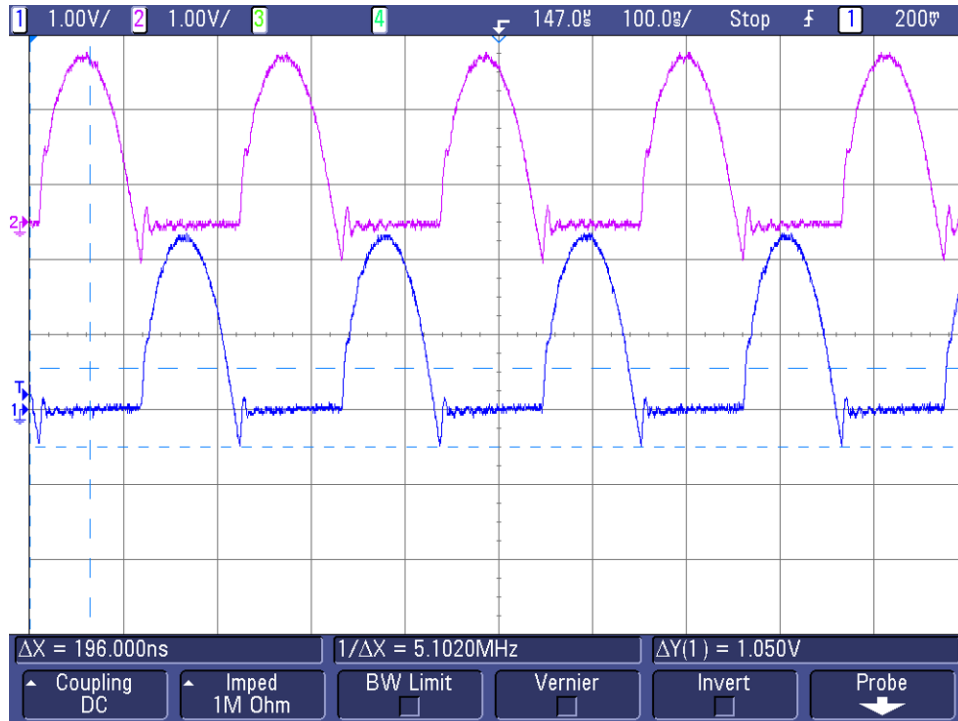
图 **16. INxA and INxB Signals Between LC Resonant Circuit and FDC2212-Q1**

3.2.3.1 Drive Current

The FDC2212-Q1 IDRIVE registers set the drive current used for each of the channels. The IDRIVE register has 5 bits that allow adjustment of this parameter between 16 µA and 1.6 mA. The registers must be set such that the sensor oscillation amplitude is between 1.2 and 1.8 V. 图 17 and 图 18 show the effect of changing the IDRIVE register on the oscillation amplitude.

Observing the change in the resonant signals in response to adjustment of the parameters of the FDC2212-Q1 registers also verifies that the communication between the microcontroller and FDC2212-Q1 is working correctly.
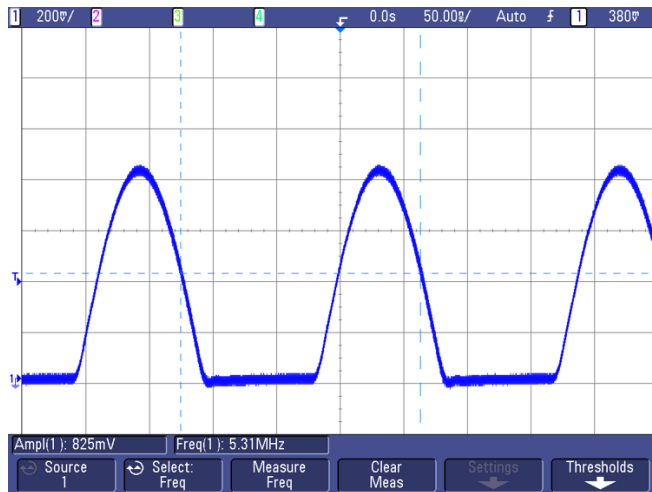
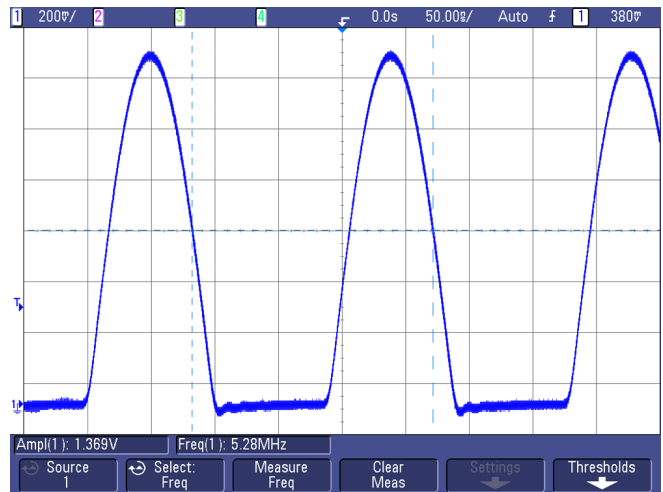图 17. Oscillation With Short Antenna and
IDRIVE = 4000

图 18. Oscillation With Short Antenna and
IDRIVE = 6000

3.2.4 Operational Kick Detection

To evaluate the function of the Capacitive Kick-to-Open design, a series of tests used hardware similar to the actual application conditions with the reference design board. Data for these tests is presented in the following sections. These tests are not intended to be complete as there are many variables that would affect any particular vehicle and situation. The test data is intended to illustrate the feasibility of this hardware to implement the basic functions of a kick-to-open system.

3.2.4.1 Kick Testing Hardware Setup

In addition to the TIDA-01409 Capacitive Kick-to-Open board and the LaunchPad microcontroller board, testing requires a 12-V power supply to take the place of the automotive battery system; this reference design operates over a wide range of input voltages and requires less than 40 mA of current from the external supply, so the requirements for a power supply are not very restrictive. Testing also requires appropriate capacitive sensors (antennas), a structure to emulate the automotive body and a method to provide kicking gestures.

To make the kicking gesture more repeatable during testing, a mechanical kicking machine, as shown in 图 19, provides the kick for each test. This mechanism provides a controlled and repeatable motion in terms of duration of kick, speed of motion, and angle of approach. The pivot point on this mechanism is about 20 inches (500 mm) above the ground, similar to the knee joint of an adult who might make the kicking gesture in the actual application. The approach of the kicking gesture is roughly a path along the circumference of an arc about the pivot point, approaching the sensor as determined by the relative placement of the sensor and the kicking mechanism. The duration of the kicking gesture made by the kicking mechanism was about 1.5 seconds in each direction, extending towards the bumper and then moving away from the bumper.

For the kicking tests which follow, the initial position of the kicking mechanism was such that the vertical distance from the bottom sensor to the kicking shoe was about 20 inches (500 cm). The final position of the standard kicking gesture was about 8 inches (200 cm) below the bottom sensor antenna. The lateral or longitudinal displacement of the kicking machine was variable, as discussed in 节 3.2.4.4.

A variety of shoes and materials can be attached to the kicking mechanism to evaluate the response do different shoes construction and material properties on the capacitive sensing. The structure of the mechanism is wood (except for the drive mechanism) so that the effect of the structure on the capacitive measurements is minimized.

图 **19. Kicking Machine With Sports Shoe**

To simulate the body of the vehicle, a bumper cover (TY04112BBQ) was mounted such that it was at a height and orientation similar to that found on a vehicle. For the purposes of initial testing, the bumper cover is kept separate from any large metal objects that would affect the capacitive measurements. Other than the license plate typically found mounted to the bumper cover, no metal structure was used in the bumper cover support. In subsequent tests, the effect of having metal in close proximity to the sensors was investigated under controlled methods.

Ford part number CJ5Z-14F680-C is a single-conductor antenna used in vehicles for kick-to-open sensing. Two of these antennas were mounted horizontally in the bumper cover as shown in 图 20. One antenna is attached near the bottom edge of the bumper cover, and the second antenna is mounted just above the license plate. Both sensors were attached to the bumper cover with adhesive tape to avoid the use of metal fasteners, which might affect the measurement results.

图 **20. Capacitive Antennas Mounted on Bumper Cover**

The entire bumper cover, sensors, and kicking mechanism were tested on a concrete floor in the loading dock area of the TI plant in Dallas, in a lab area as close as possible to the actual conditions of a garage or parking lot.

3.2.4.2   Background Measurements

The first step is to determine the measurement precision and expected measurement variation due to background noise. For the sensor measurements which follow, the sampling rate is 50 ms/sample or 20 samples per second, unless otherwise noted.

From 图 21, the peak-to-peak measurement variation is on the order of 600 counts (33114150 – 33113550 = 600). This is a very small variation with respect to the offset (around 33 million counts).
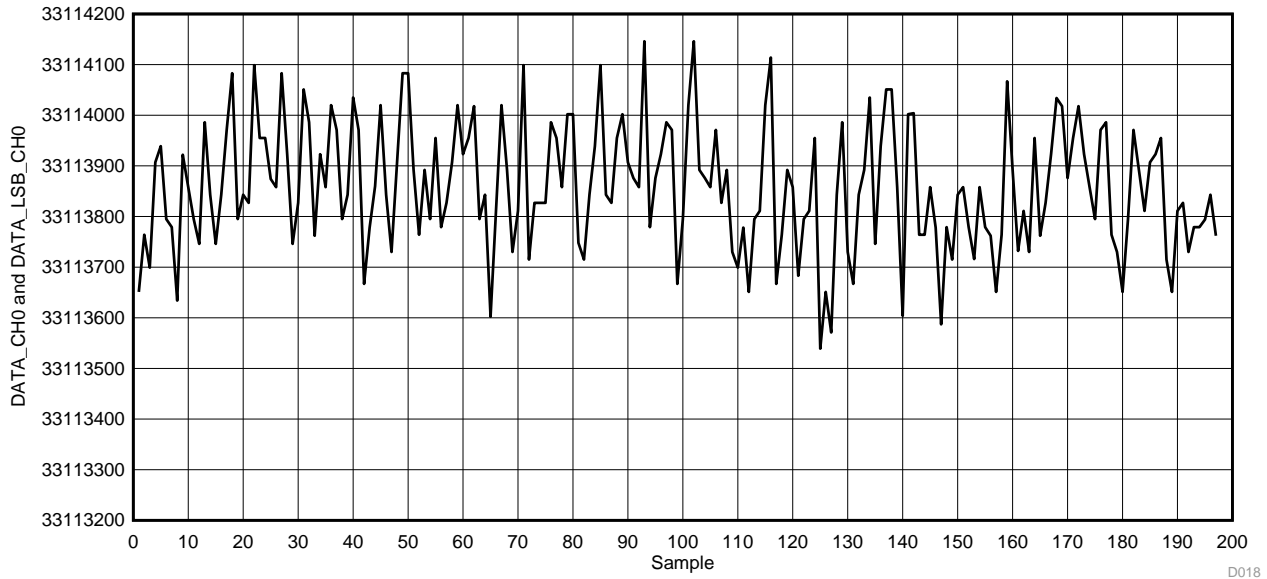
图 **21. Measurements With No Kicking Gesture**

3.2.4.3   *Response to Standard Kick*

From 图 22, the peak change due to a standard kick is about 16,000 counts (33,116,000 – 33,100,000 = 16,000). Therefore, the kick measurement amplitude is over 25 times as large as the peak-to-peak measurement variation. In terms of signal-to-noise ratio, this can be expressed as S/N = 20 × log10 (16,000 / 600) = 28.5 dB.
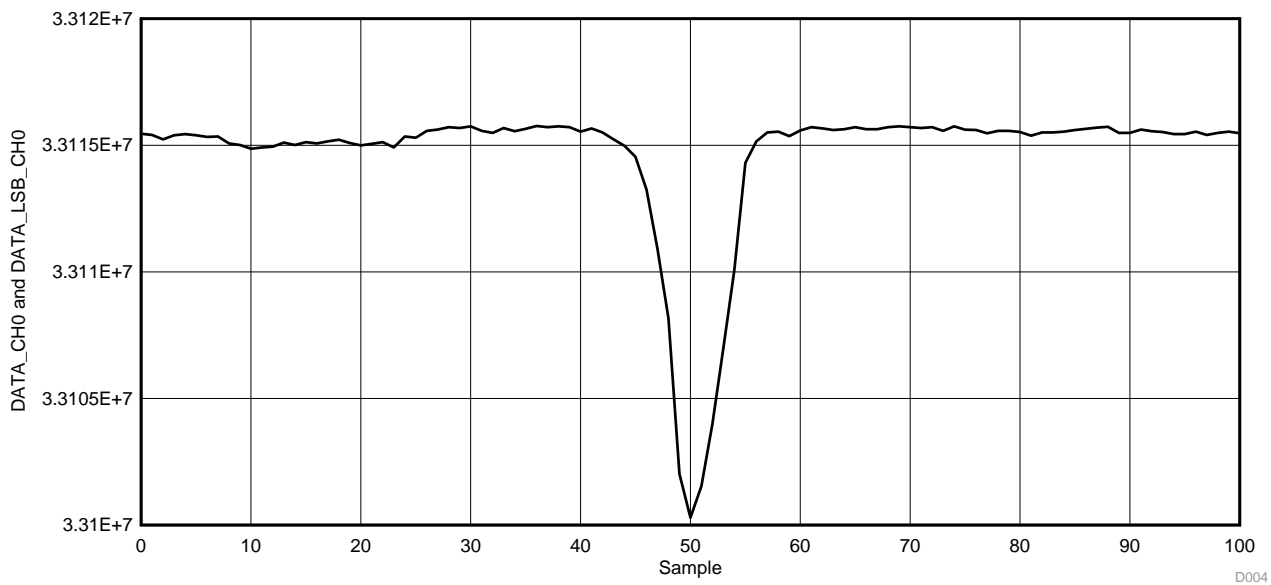
图 **22. Measurement of Standard Kicking Gesture**

3.2.4.4 *Response to Longitudinal Displacement*

图 23 shows three successive standard kicking gestures displaced 6 inches (15 cm) from center towards the right side of the bumper. The magnitude of the kick is about 32.168 million counts minus 32.1565 million counts, or about 11500 counts. Although there is some variation in the magnitude, these measurements are fairly consistent for all three kicks.
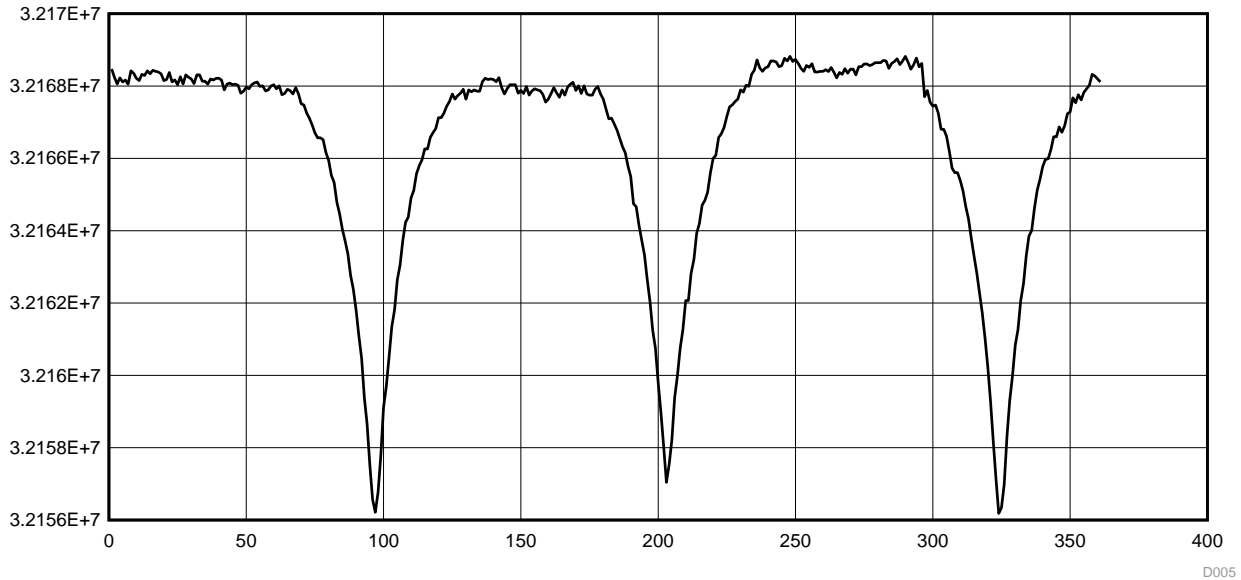

图 23. Three Kicks 6 Inches to Right of Center

图 24 shows three successive standard kicking gestures displaced 10 inches (25 cm) from center towards the left side of the bumper. The magnitude of the kick is about 32.175 million counts minus 32.166 million counts, or about 9000 counts. Although there is some variation in the magnitude, these measurements are fairly consistent for all three kicks.

图 25 shows three successive standard kicking gestures displaced 20 inches (25 cm) from center towards the right side of the bumper. The magnitude of the kick is about 33.111 million counts minus 33.1086 million counts, or about 2400 counts. Although there is some variation in the magnitude, these measurements are fairly consistent for all three kicks.
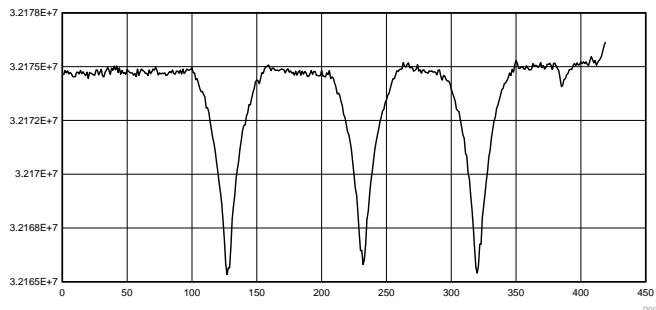
图 **24. Kicks 10 Inches Away From Center of Antenna**
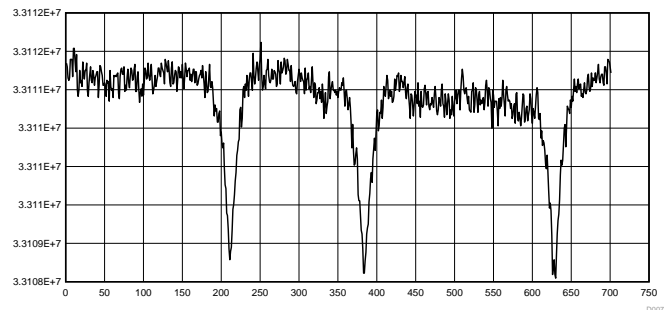
图 **25. Kicks 20 Inches Away From Center of Antenna**

These figures show that the amplitude of the kick signal decreases as the location of the kick is displaced longitudinally away from the center of the capacitive antenna. This is summarized in 图 26 where the kick response magnitude is plotted in decibels versus the location of the kick.
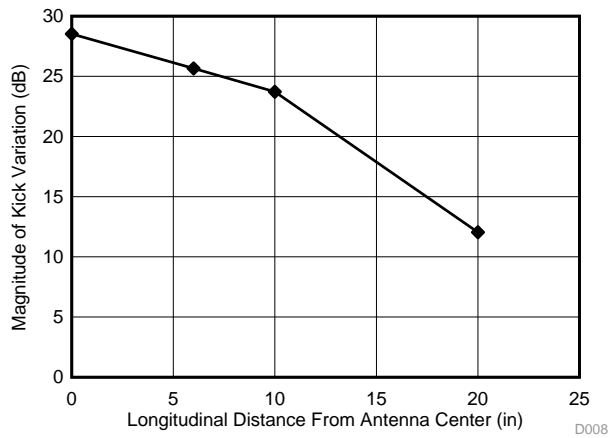
图 **26. Kick Response versus Longitudinal Displacement From Center**

3.2.4.5   *Impact of Electrical Properties of Kicking Object*

The amplitude of the sensor response to a kicking gesture depends on the electrical properties of the kicking object. 图 27 illustrates this effect, showing a plot of the sensor response to a series of kicking gestures with only the electrical properties of the shoe being changed. The response of both the lower antenna (DATA0) and the upper antenna (DATA1) are shown. The left half of the plot shows the response to a series of three standard kicks by the kicking mechanism with a normal sports shoe. The right half of the plot shows the response to a series of three standard kicks by the kicking mechanism with a test wire (typical 1 meter bench test lead) attached along the length of the shoe on the kicking mechanism.
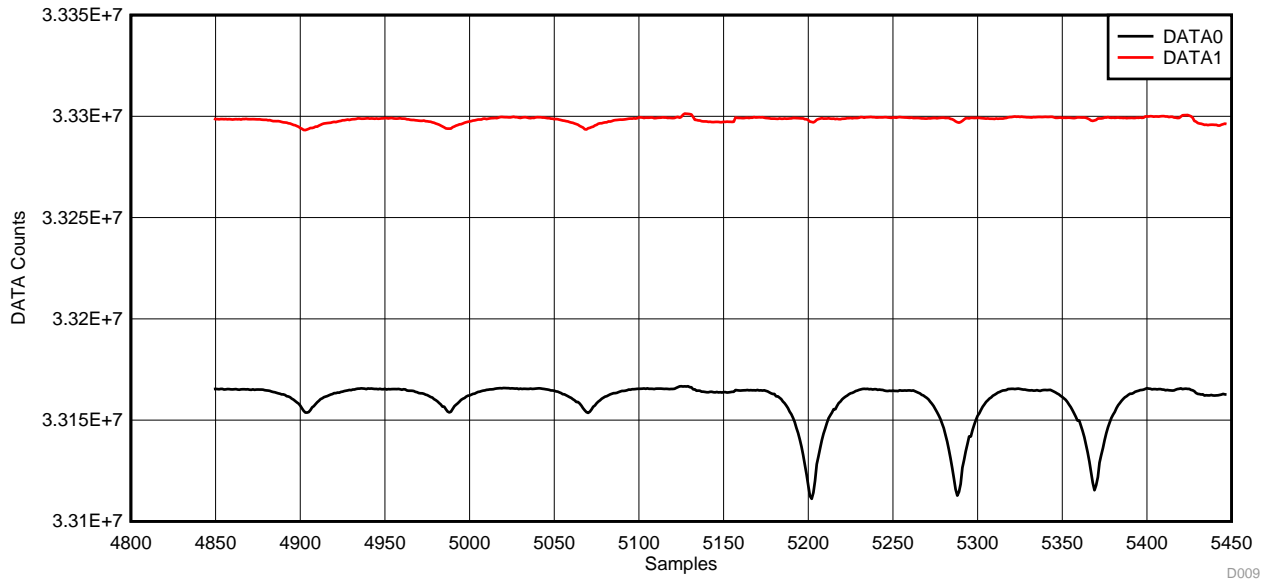
图 **27. Three Standard Kicks With Sports Shoe, Followed by Three Standard Kicks by Sports Shoe With Attached Test Wire**

The response of DATA0, the sensor data from the lower sensor antenna, to the kicks with the attached wire is much more significant in amplitude compared to the kicks without the wire. This indicates that gestures made with shoes containing higher quantities of conductive metal can be expected to have a higher response amplitude than shoes with a low quantity of metal.

3.2.4.6   *Vertical Discrimination Using Two Sensor Antennas*

The use of two capacitive antennas allows discrimination of approaching objects in terms of orientation from above or below. With the two antennas mounted on the bumper cover as shown in 图 20, the response from each antenna is significantly different for objects approaching from the top or from the bottom direction.
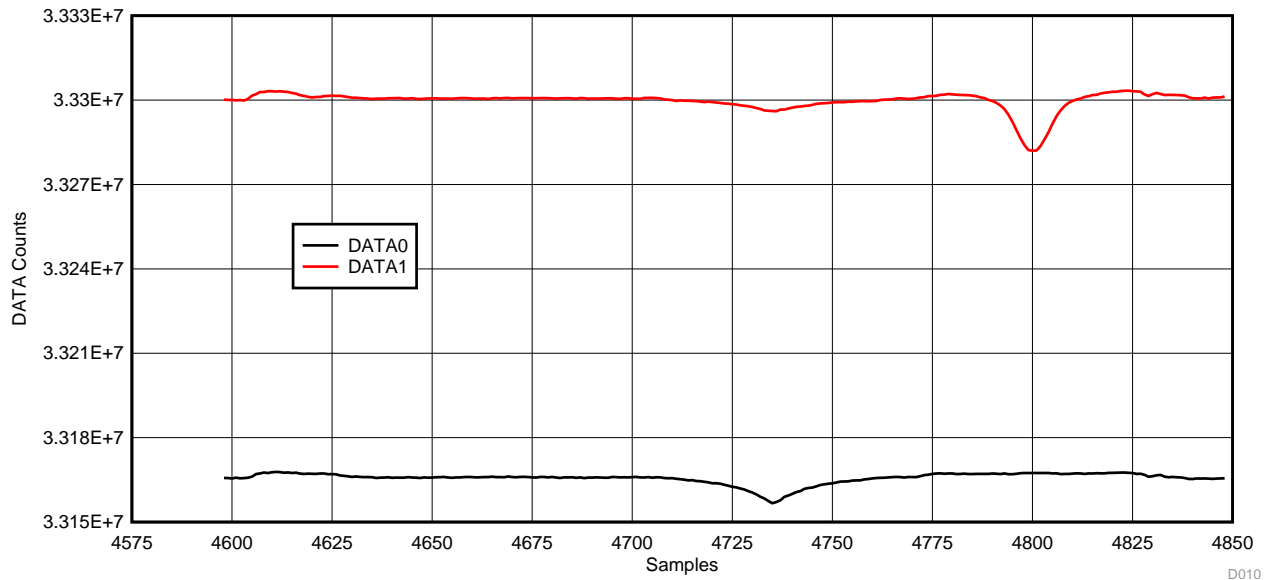

图 **28. Kick Gesture From Below Followed by Hand Gesture From Above**

图 28 shows the difference in response for the bottom antenna (DATA0) and the top antenna (DATA1) for objects approaching from below the bumper and approaching from above the bumper. As expected, the response of the lower antenna is much more pronounced that the response of the upper antenna for objects approaching from the bottom. Similarly, the response of the upper antenna is much more pronounced than the response of the lower antenna for objects approaching from above.

The disparity of the size of responses can be attributed to the non-standard gesture from above the sensors; a simple gesture with an approaching hand was made to demonstrate the qualitative effect of the spatial orientation of the antennas.

This ability to determine the direction of approach for an object or a gesture is useful to avoid incorrectly activating the closure mechanism when an operator is opening the trunk manually, or putting objects into the trunk from above the bumper, or similar gestures that do not indicate a desire to have the kick-to-open feature activate.

3.2.4.7 *Effect of Metal Near Antennas*

The capacitive sensing solution is affected by nearby conductive metals. 图 29 shows the effect of placing a 5 kg piece of steel (a bench vise) right next to the capacitive antenna. In this case, the 5 kg piece of steel was not grounded, but was simply placed on the plastic bumper cover on which the antennas are mounted. There is a shift of in the background measurements from about 33.17 million counts to about 32.92 million counts, or a shift of about 250,000 counts, or about 0.75% of the original measurement. Compared to the measurements during a kick gesture, this shift is very significant, at least 10 times larger than the standard kick measurement amplitude.

However, the measurements for the kick gestures, three before the steel was added, and three kicks after the steel was added, appear to show similar response in terms of the amplitude of the measurements during the kicking gesture. This indicates that while the introduction of metal close to the antennas causes a shift in the measurements, the sensitivity of the system to kicking gestures is not significantly impacted.
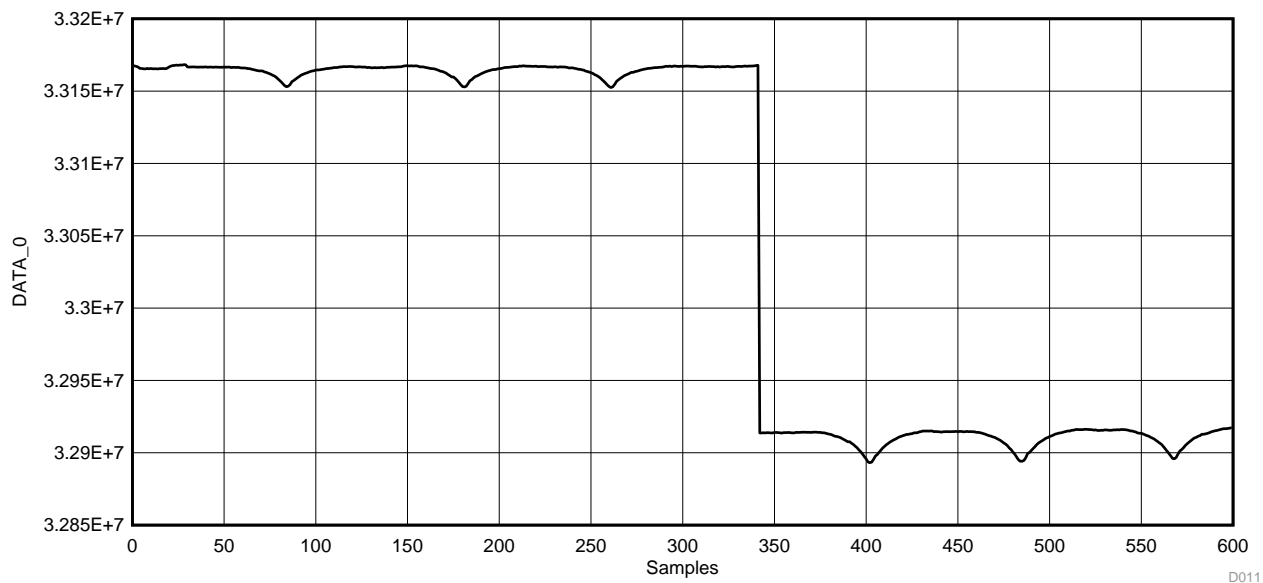
图 29. Three Standard Kicks Towards Standard Bumper Cover, Followed by Three Standard Kicks Towards Bumper Cover With Ungrounded 5 kg Steel in Close Proximity

In the previously described test, the steel introduced during the test was not grounded, but simply put in close proximity to the sensor antennas. To determine the effect of grounding an added piece of metal to the test environment, the above test was repeated, with an electrical connection between the added 5-kg steel and the common ground (GND) of the sensor electronics.

图 30 shows the overall effect of the addition of a 5 kg piece of grounded steel to the immediate proximity of the sensor antenna. As was seen in the ungrounded steel case, there is a significant shift in the DATA0 measurements from the sensor. Comparing with the previous case, the shift is much larger in amplitude, shifting from about 3.29 MHz to about 3.15 MHz, a shift of about 4%. The shift is large enough that the response to the kicking gestures is not recognizable in the scale of the plot.
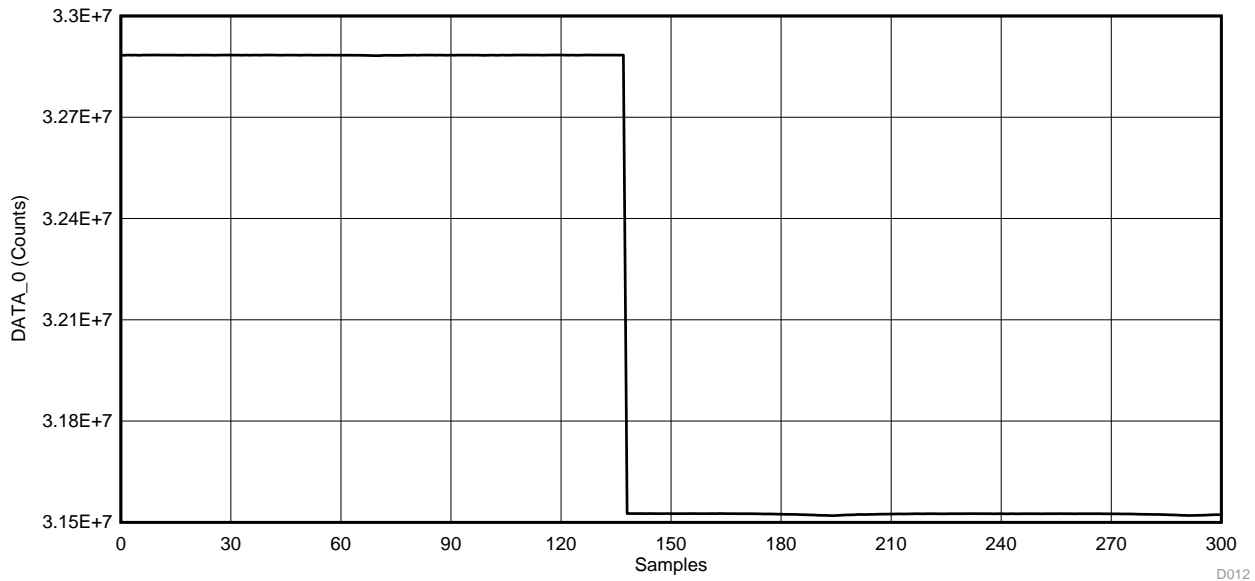

D012

图 30. Shift in Measurements When Grounded 5-kg Steel is Placed in Close Proximity to Antenna

A plot of the DATA0 measurements after the shift has occurred (the horizontal scale has reset to show only the samples starting with sample 150 from 图 30) is shown in 图 31. Here, the response to the three kicking gestures is obvious, with an amplitude of about 5500 counts.

D013
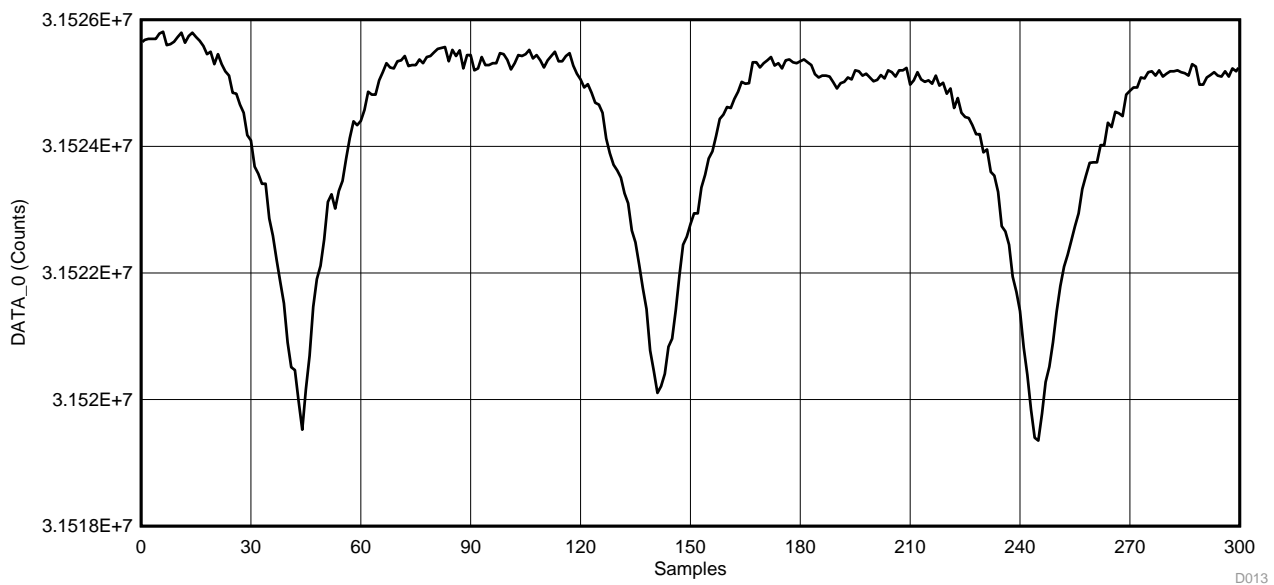
图 31. Sequence of Three Standard Kicks With Grounded 5-kg Steel in Close Proximity Antenna

3.2.4.8 *Wet Conditions*

One environmental consideration for automotive kick-to-open applications is water on the system due to driving in wet conditions, either rain, snow, or simply puddles on the road. To mimic the effects of a wet environment, the test components (antennas and surrounding bumper) were sprayed with ordinary tap water. 图 32 shows the test hardware after being sprayed with water.

图 **32. Wet Capacitive Antenna**

图 33 and 图 34 show the data samples from the FDC2212-Q1 with standard kick gestures for both dry conditions and then with the test hardware sprayed with water. For the dry conditions, the DATA_0 is about 33.082 million counts before and after the kick, and the minimum DATA_0 drops to about 33.068 million counts during the kick gesture. This gives a measured kick amplitude of about 14,000 counts during dry conditions.

For the wet conditions, DATA_0 is about 33.076 million counts before and after the kick, and the minimum DATA_0 drops to about 33.062 million counts during the kick gesture. This gives a measured kick amplitude of about 14,000 counts for the wet conditions, very similar to the dry condition measurements.
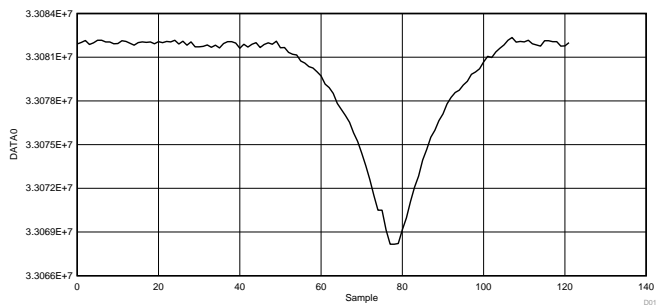
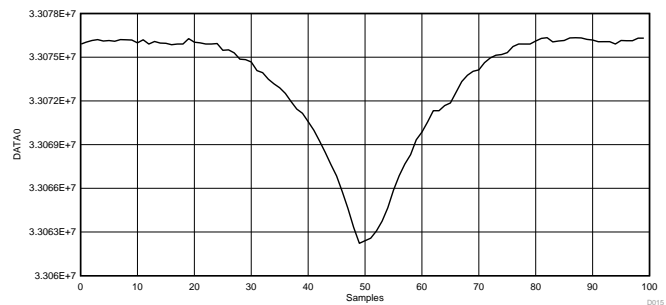图 **33. Standard Kick Towards Dry Antenna, Center of Bumper**

图 **34. Standard Kick Towards Wet Antenna, Center of Bumper**

As seen in these figures, there is a slight shift in the background level from the dry to wet conditions, but there is not a significant difference in the amplitude of the measurements for the kicking gesture itself.

3.3   *Response to Other Objects*

Of interest in kick-to-open systems is the response of the sensor to objects that may move under the bumper, such as small animals, toys, and balls, or rolling dropped objects such as groceries. In these cases, the kick-to-open system ideally would be able to discriminate between these objects moving under the bumper and a valid kicking gesture.

图 35 through 图 38 show the response of the capacitive kick-to-open via the lower capacitive sensor to a few foreign objects moving under the test bumper set-up. For a basis of comparison, 图 35 shows the output of the capacitive sensor system when no object is under the bumper. The amplitude of the variation is about 600 counts peak-to-peak.

图 36 shows the response with a stuffed animal, about the size of a cat, moving under the bumper sensors. Starting with sample 100, the DATA_0 counts shift by about 300 counts, until sample 160. This indicates the stuffed animal, which was used as a simulation of an actual animal, caused a slight response, but the signal to noise ratio for this response was relatively low.

A soccer ball was rolled under the bumper capacitive sensor, and the response captured as shown in 图 37. The DATA_0 signal shows a brief excursion from the normal background variation, with a sharp peak at about sample 72. The amplitude of the response to a rolling ball is about 400 counts. As with the stuffed animal, the signal-to-noise ratio of this event is not very high.

图 38 shows the response to a small can filled with condensed soup rolling under the bumper. In this case, the response is not distinguishable from the typical background variation. Therefore, this event does not seem likely to cause a false triggering of the capacitive kick-to-open system.
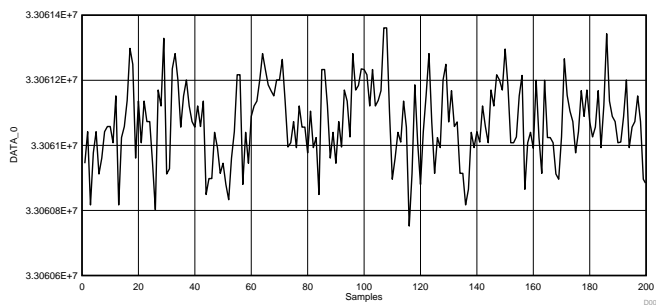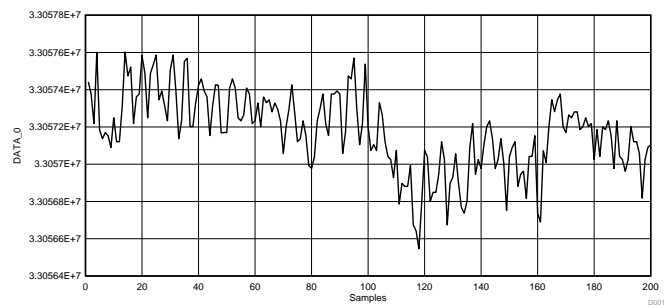
图 35. Response With No Object Under Bumper
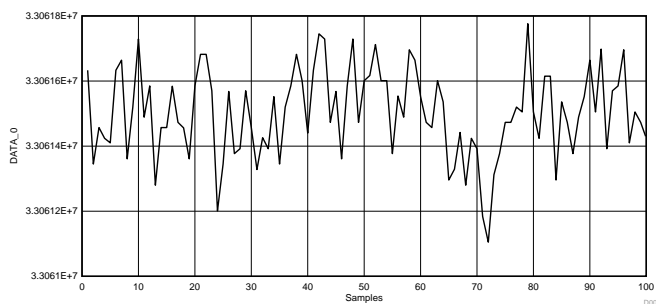
图 36. Response to Stuffed Animal Moving Under Bumper
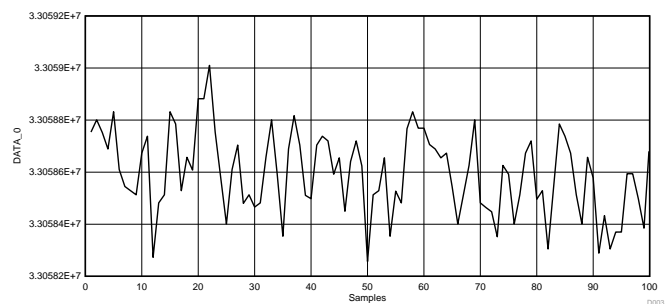
图 37. Response to Ball Rolling Under Bumper

图 38. Response to Can Rolling Under Bumper

4   Design Files

4.1   Schematics

To download the schematics, see the design files at TIDA-01409.

4.2   Bill of Materials

To download the bill of materials (BOM), see the design files at TIDA-01409.

4.3   PCB Layout Recommendations

4.3.1   Form Factor

The overall dimensions and connector placement of the TIDA-01409 Capacitive Kick-to-Open board were constrained by the LaunchPad and BoosterPack connectors, which connect the LaunchPad microcontroller board to the TIDA-01409 board. As shown in 图 39, the width (horizontal or X-dimension) of the TIDA-01409 board is slightly wider than distance between the two 10-pin connectors J2 and J3. The centerline of these connectors is 1.8 inches, determined by the LaunchPad standard, and the width of the board is 2 inches. Likewise, the length (vertical or Y-dimension) is slightly longer than the length of each 10-pin connector; the pin spacing of these connectors is 0.1 inch, so the overall length of each connector is approximately 1 inch, and the length of the TIDA-01409 is 1.2 in the Y dimension.
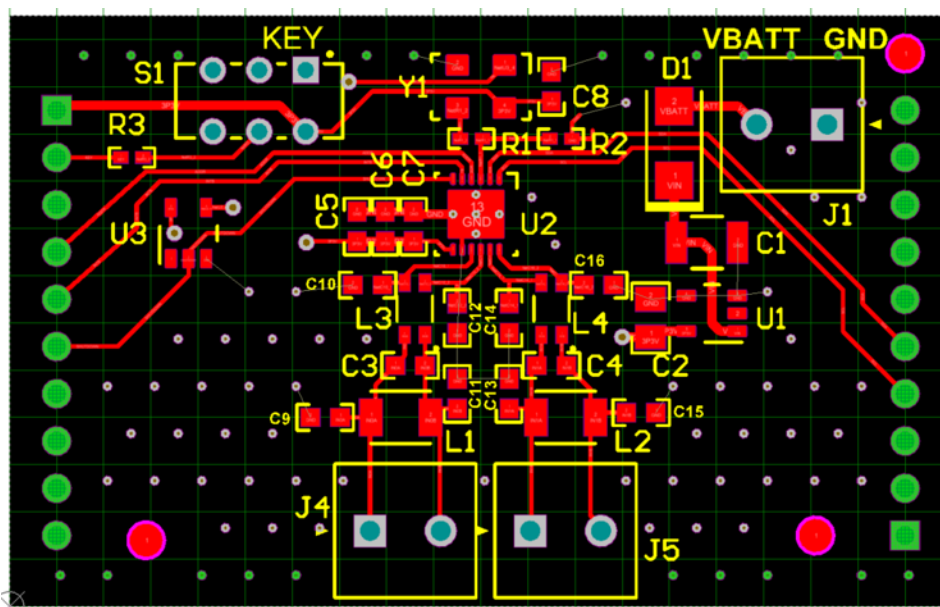

图 **39. Overview of TIDA-01409 Layout (Top View)**

图 40 and 图 41 show the arrangement of components on the top and bottom side of the TIDA-01409 board. The board size is primarily dictated by the size and spacing of the BoosterPack connectors (J2 and J3), which interface to the LaunchPad microcontroller board. Connections to the sensors are through terminal blocks J4 and J5. Connection to the 12-V automotive battery system is through terminal block J1. Switch S1 is a manual slide switch that allows setting the state to "key fob detected" or "no key fob detected" to emulate input from the vehicle security system.

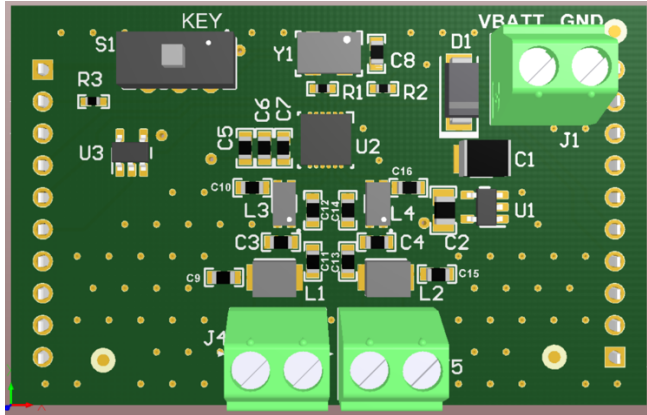There are no components on the bottom of the board except the connectors J2 and J3.

图 **40. Top View of TIDA-01409 Board Showing Component Placement**

图 **41. Bottom View of TIDA-01409 Board**

4.3.2 Input Power Placement and Routing

The power supply for the TIDA-01409 is not high voltage, and the current consumption is relatively small. However, attention to the placement of components and routing for the input power reduces concerns about coupling between the battery voltage and the sensor signals. 图 42 shows the placement of the input connector J1 with the VBATT connected directly from J1-2 to the anode of D1. The cathode of D1 is routed directly to the input pins of the TPS7B6933-Q1 voltage regulator, with input capacitor C1 and output capacitor C2 very close for regulator stability without external signal interference. Because the currents for this system are relatively low, the power traces are only slightly wider than the default 10-mil thickness. In this view, the surrounding ground plane has been hidden for clarity.
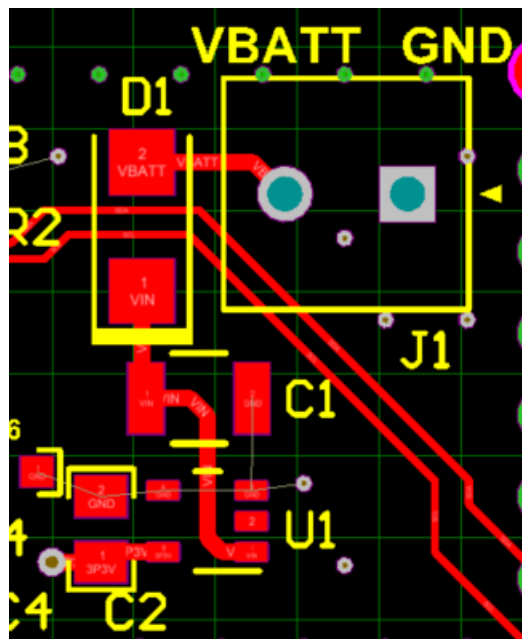

图 **42. Input Power (VBATT) Routing and Component Placement (Top Side)**

4.3.3 3.3-V Supply Routing

The routing of the 3.3-V supply (signal 3p3V) is highlighted in 图 43. In this view, traces on the top layer are red, and traces on the bottom layer are blue. The source of the 3.3-V supply is U1 on the right side of the board; the supply is distributed to the FDC2212-Q1, to the LaunchPad microcontroller board through J2-1, to the logic inverter U3, to the oscillator Y1 and to the manual switch S1. The routing of the 3p3V traces avoids the resonant circuit, which is placed towards the bottom edge of the board, to avoid coupling from the resonant circuit to the power supply. Decoupling capacitors C5, C6, and C7 are located near the central distribution point to reduce any current spike throughout the signal.
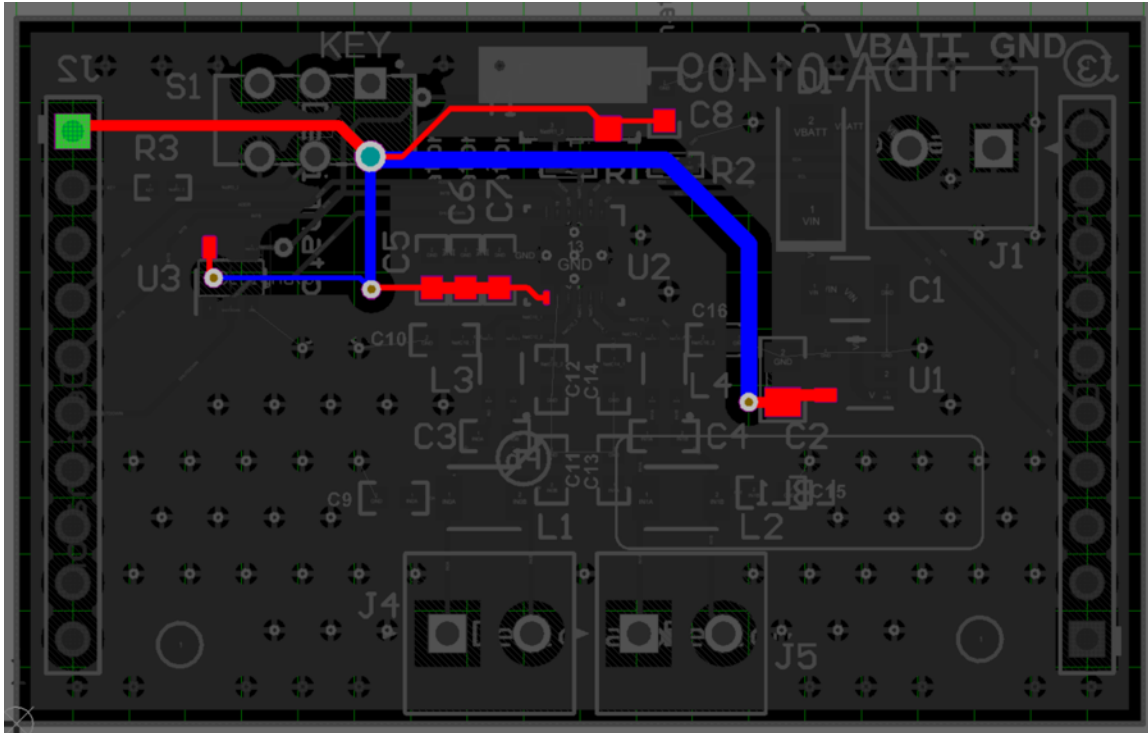

图 **43. 3.3-V Supply Routing on TIDA-01409 Board (Top View)**

4.3.4 Capacitive Sense Routing

图 44 shows the routing and layout for the capacitive sensor circuits, including the FDC2212-Q1 Capacitive-to-Digital Converter and the resonant circuit components. The two channels of resonant circuit components are placed between the FDC2212-Q1 (U2) and the connectors J4 and J5, which connect to the sensor antennas. The component placement for the two channels is symmetric and maintains straight paths from the excitation source (the FDC2212-Q1) through the inductor-capacitor resonant circuit to the connectors.

There are several components that are not installed unless issues with EMC are observed, for example C10 and C12. The traces to these components is kept short to reduce the effect of any stubs, thereby reducing the concern for undesirable transmission line effects. In 图 44, the surrounding ground plane has been hidden for clarity.

图 **44. Capacitive-to-Digital Converter and Resonant Circuit Component Placement and Routing**
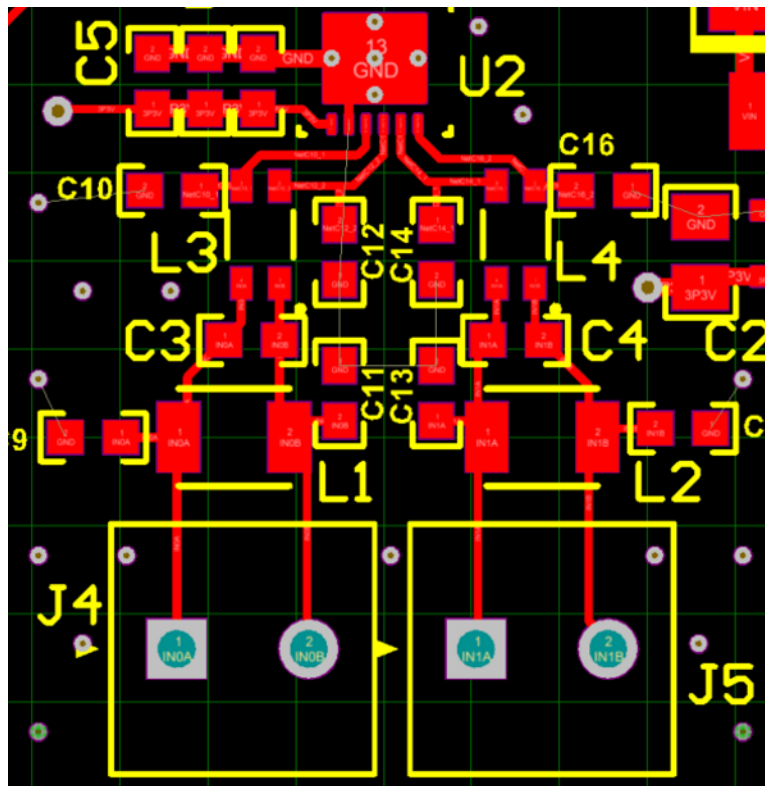
4.3.5 Layout Prints

To download the layer plots, see the design files at TIDA-01409.

4.4 Altium Project

To download the Altium project files, see the design files at TIDA-01409.

4.5 Gerber Files

To download the Gerber files, see the design files at TIDA-01409.

4.6 Assembly Drawings

To download the assembly drawings, see the design files at TIDA-01409.

5   Software Files

To download the software files, see the design files at TIDA-01409.

6   Related Documentation

1. Texas Instruments, *Multi-Channel 28-Bit Capacitance-to-Digital Converter (FDC) for Capacitive Sensing*, FDC2112-Q1 Datasheet (SNOSCZ9)
2. Texas Instruments, *FDC2114 and FDC2214 EVM User's Guide* (SNOU138)
3. Texas Instruments, *Capacitive Proximity Sensing Using FDC2x1y* , Application Report (SNOA940)
4. Texas Instruments, *High-Voltage Ultra-Low IQ Low-Dropout Regulator* , TPS7B6933-Q1 Datasheet (SLVSCJ8)
5. Texas Instruments, *Single Inverter Gate*, SN74LVC1G04-Q1 Datasheet (SCES482)
6. Texas Instruments, *Using the USCI I²C Master*, Application Report (SLAA382)
7. Texas Instruments, *MSP430x2xx Family User's Guide* (SLAU144)

6.1   商标

LaunchPad, BoosterPack, MSP430, Code Composer Studio, C2000 are trademarks of Texas Instruments. All other trademarks are the property of their respective owners.

7   About the Author

CLARK KINNAIRD is a systems applications engineer at Texas Instruments. As a member of the Automotive Systems Engineering team, Clark works on various types of end-equipment, especially in the field of body electronics, creating reference designs for automotive manufacturers. Clark earned his bachelor of science and master of science in engineering from the University of Florida, and his Ph.D. in electrical engineering from Southern Methodist University.

有关 TI 设计信息和资源的重要通知